Hybrid interval and random analysis for structural-acoustic systems including periodical composites and multi-scale bounded hybrid uncertain parameters

Ning Chen[1,*], Siyuan Xia[1], Dejie Yu[1], Jian Liu[1], Michael Beer[2,3,4]

[1]State Key Laboratory of Advanced Design and Manufacturing for Vehicle Body, Hunan University, Changsha, Hunan, 410082, People's Republic of China

[2] Institute for Risk and Reliability, Leibniz University Hannover, Callinstr. 34, 30167 Hannover, Germany

[3] Institute for Risk & Uncertainty, School of Engineering, University of Liverpool, Brodie Tower, Brownlow Street, Liverpool L69 3GQ, United Kingdom

[4] School of Civil Engineering & International Joint Research Center for Engineering Reliability and Stochastic Mechanics (ERSM), Tongji University, China

Abstract: For the response analysis of periodical composite structural–acoustic systems with multi-scale uncertain-but-bounded parameters, a bounded hybrid uncertain model is introduced, in which the interval variables and the bounded random variables exist simultaneously. In the periodical composite structural-acoustic system, the equivalent macro constitutive matrix and average mass density of the

∗ Corresponding author. Tel.: +86 731 88821915; fax: +86 731 88823946.
E–mail address: chenning@hnu.edu.cn (Ning Chen)

microstructure are calculated through the homogenization method. On the basis of the conventional first-order Taylor series expansion, a homogenization-based hybrid stochastic interval perturbation method (HHSIPM) is developed for the prediction of periodical composite structural-acoustic systems with multi-scale bounded hybrid uncertain parameters. By incorporating the Gegenbauer polynomial approximation theory into the homogenization-based finite element method, a homogenization-based Gegenbauer polynomial expansion method (HGPEM) is also proposed to calculate the bounds of expectation and variance of the sound pressure response. Numerical examples of a hexahedral box and an automobile passenger compartment are given to investigate the effectiveness of the HHSIPM and HGPEM for the prediction of periodical composite structural-acoustic systems with multi-scale bounded hybrid uncertain parameters.

Key Words：Gegenbauer polynomials; Structural-acoustic system; Homogenization method; Periodical composites; Bounded hybrid uncertain model

1. Introduction

In recent years, composite materials have been widely applied in the military industry and construction industry, especially, in the vehicular and aviation industry owing to its lightweight, high strength and tenacity features. However, when excited by a harmonic force, the flexible and lightweight composite panels are vulnerable to vibration and can radiate noise into passenger compartment. In particular, when the harmonic exciting frequency is close to the inherent frequency of composite panels or the acoustic cavity of the passenger compartment, the resonant noise generated by the

composite panels is beyond sufferance. Therefore, conducting the vibro-acoustic analysis of composite structural-acoustic systems is very worthwhile and meaningful.

With the rapid development of researches on the analyses of structural-acoustic systems, a lot of numerical approaches have been proposed. The coupled finite element method/finite element method (FEM/FEM) is the most commonly used one among these approaches for structural-acoustic systems in engineering practice. In the coupled FEM/ FEM, both the structure domain and the fluid domain are simulated by FEM models. However, the key point of solving the composite structural-acoustic problem is to analyze the composite material firstly at micro-scale before calculating the response of the structural-acoustic system at macro-scale. Generally, a composite material has a complicated microstructure and various constituents, which can lead to the inherent characteristics of composite materials, such as strong heterogeneity and anisotropy [1-2]. Through the homogenization method which is based on an asymptotic expansion of the governing equations, the effective parameters of the heterogeneous composite material can usually be induced [3-5]. In this way, the heterogeneous medium is transformed into an equivalent material model which is energetically equivalent to the heterogeneous medium. By integrating the homogenization method with the coupled FEM/FEM, the homogenization-based finite element method (HFEM) is proposed for the prediction of periodical composite structural–acoustic systems [6]. In the HFEM, the bi-material solid isotropic material with penalization model is employed to describe the material distribution of the microstructure [7].

Traditional numerical methods for the dynamic analysis of the vibration and noise issues are mainly based on deterministic geometric, material and physical parameters. However, uncertainties related to these parameters are unavoidable in practical engineering due to the effects of aggressive environment factors, inevitable manufacturing errors and incomplete knowledge [8-10]. The analysis results may be unreliable without considering those uncertainties involved in the system. In this context, increasing attention has been gained on the uncertain analysis of structural-acoustic systems in recent years. Until now, Xia et al. have developed numerical approaches for the response analysis of structural-acoustic systems with interval parameters, hybrid random and interval parameters, and hybrid interval random parameters [11-13]. The uncertainty propagation in SEA (Statistic Energy Analysis) for structural-acoustic coupled systems with uncertain-but-bounded parameters has been investigated by Xu et al. [14]. Yin et al. have focused on the analysis of structural-acoustic systems with interval parameters at the mid-frequency range through hybrid finite element/statistic energy method [15]. A new random interval method for response analysis of structural–acoustic system with interval random variables has been proposed by Xia et al. [16]. Uncertainty analysis of a structural-acoustic problem with imprecise probabilities has been conducted by Chen et al. based on p-box representations [17]. Yin et al. have proposed a unified method for the interval and random analysis of structural–acoustic system with large uncertain-but-bounded parameters [18]. Hybrid uncertainty propagation in structural-acoustic systems has been studied by Xu et al. based on the polynomial

chaos expansion and dimension-wise analysis [19]. Though a variety of researches on uncertainty analysis of the structural-acoustic system have been done, all of these aforementioned researches are limited to structures consisted of isotropic material and the considered uncertainties are confined to macro-scale. As for periodical composite structural-acoustic systems, multi-scale uncertainties exist simultaneously. At the micro-scale, the uncertainty may come from the constituent material properties of the microstructure due to manufacturing errors. The source of the uncertainties at the macro-scale is from the physical parameters of the acoustic medium and the external load resulting from the environment. Both the uncertainties from the micro-scale and the uncertainties from the macro-scale can have an effect on the frequency response of the periodical composite structural-acoustic system. Thus, multi-scale uncertainties should be considered when analyzing periodical composite structural-acoustic systems. Recently, Chen et al. have conducted the interval analysis for periodical composite structural-acoustic problem with multi-scale uncertain-but-bounded parameters based on perturbation method [6]. However, the proposed interval analysis approach inherits the drawback of the perturbation method, which limits its application in periodical composite structural-acoustic problem with small multi-scale uncertain level. Overall speaking, researches on periodical composite structural-acoustic systems with considering multi-scale uncertainties are promising but rarely reported.

To deal with the randomness, various probabilistic approaches have been developed, such as the Monte Carlo method (MCM) [20-21], the random perturbation

method [22-25], the random orthogonal polynomial approximation method [26-29] and so on. However, the premise of these probabilistic approaches is that the detailed probability distribution of uncertain parameters is provided [30-31]. Unfortunately, the information to construct the probability density function (PDF) is not always sufficient or is sometimes very difficult to acquire. To overcome the shortcoming of probabilistic approaches, interval approaches provide an appropriate alternative to cope with the uncertain modeling with limited information [32]. In the interval approach, the interval variable is employed to model the uncertain parameter whose lower and upper bounds are well defined but information about its probability density functions is missing. The scanning method, the perturbation method [11,33] and the orthogonal polynomial approximation method can be used for interval analysis [14,34]. The probability approach and the interval approach are appropriate for the uncertain problems with random variables and interval variables respectively. However, sometimes the random variables and interval variables may exist simultaneously in an uncertain system. In this situation, a hybrid uncertain model is proposed by Elishakoff and Colombi [35]. In the hybrid uncertain model, the random variables are used to describe the uncertain parameters with sufficient information to determine the probability distributions, whereas, the interval variables are used to represent the uncertain parameters without sufficient information to construct the precise probability distributions. The hybrid uncertain model inherits the merits of both random model and interval model and has been widely applied in many engineering fields [36-38]. Several hybrid uncertain numerical methods are

developed on the basis of the perturbation method, MCM and polynomial approximation method [12,39-41]. However, due to the manufacturing tolerance design, it has been deemed that the associated uncertain parameters are always bounded in real engineering practice. Naturally, a bounded hybrid uncertain model can be formulated, in which the variation ranges of both the interval variables and random variables are defined strictly. Such bounded hybrid uncertain model is of particular practical application value when manufacturing tolerance is considered. Therefore, a bounded hybrid uncertain model is introduced herein to treat the multi-scale uncertainties in the periodical composite structural-acoustic system. To date, the problem of periodical composite structural-acoustic system has not yet been approached with multi-scale bounded hybrid uncertainties.

For the periodical composite structural-acoustic system with multi-scale bounded hybrid uncertainties, there is no doubt that the integration of MCM and scanning method is the most straightforward approach. However, the accuracy of this integrated method depends on the number of samples. Generally, this integrated method is regarded as a reference approach for validating the accuracy of other methods due to its excessive computational burden. To circumvent the excessive computational burden of the integration of MCM and scanning method, the versatile perturbation method can be employed to develop a desirable hybrid analysis approach. Usually, the first-order Taylor expansion is adopted in the hybrid uncertain perturbation-based method because of its simplicity and computational efficiency. Therefore, based on the first-order Taylor expansion, a homogenization-based hybrid stochastic interval

perturbation method (HHSIPM) is developed to predict the periodical composite structural-acoustic system with multi-scale bounded hybrid uncertainties in this paper. Since the response of periodical composite structural-acoustic system is a strong non-linear function in terms of the input parameters at micro-scale, the HHSIPM has its own defect that it is limited to a bounded hybrid uncertain periodical composite structural-acoustic problem with small uncertain level. Under this circumstance, the polynomial approximation method is a good alternative, which can be used to handle the bounded hybrid uncertain problems with large uncertain level. A new hybrid method by integrating Polynomial Chaos expansion and Chebyshev interval expansion is developed to predict the dynamic response of vehicle systems [41]. For acoustic problem with large hybrid uncertain-but-bounded parameters, an orthogonal polynomial approximation method is proposed by Yin et al. [18,42], in which a derivative λ-PDF model based on Gegenbauer polynomial expansion is employed. Compared with the traditional orthogonal polynomial approximation methods in probabilistic analysis, the advantage of the derivative λ-PDF model is that it can approximate any mono-peak or mono-valley PDFs. Furthermore, the Gegengauer polynomial expansion method has a better accuracy than the perturbation method in interval analysis, and the efficiency of the Gegengauer polynomial expansion method is much greater compared with the scanning method [18]. From an overall perspective, the Gegenbauer polynomial approximation method can play a good role in dealing with the bounded hybrid uncertain problem. Hence, it is herein introduced to the uncertain analysis of the periodical composite structural-acoustic system with

multi-scale bounded hybrid uncertain parameters. By integrating the Gegenbauer polynomial expansion with the HFEM, a homogenization-based Gegenbauer polynomial expansion method (HGPEM) is developed for the periodical composite structural-acoustic system with multi-scale bounded hybrid uncertain parameters.

The remainder of this paper is organized as follows. In Section 2, the HFEM for the periodical composite structural-acoustic system is briefly presented. Section 3 introduces the bounded hybrid uncertain model. In Section 4 and Section 5, the HHSIPM and HGPEM for periodical composite structural-acoustic system with multi-scale bounded hybrid uncertainties are developed respectively. Two numerical examples are given to investigate the effectiveness and accuracy of the proposed methods in Section 6 and conclusions are drawn in Section 7.

2. The homogenization-based finite element method (HFEM) for the periodical composite structural-acoustic systems

This paper examines a case in which a plate constructed with periodic microstructures is coupled with an acoustic cavity. The microstructure is assumed to have the identical configuration and uniform distribution within the macroscopic domain. The micro unit cell is considered to be constituted of two different solid isotropic materials. Both the plate and the acoustic medium satisfy the linear constitutive equations and the acoustic medium is assumed to be inviscid and incompressible. On the interface between the plate and the acoustic medium, only the normal displacement of the plate is coupled with the acoustic medium and the acoustic medium just exerts normal loads on the plate in return.

The effective macro constitutive matrix $\boldsymbol{D}^{\mathrm{H}}$ of periodical composites can be calculated based on homogenization method [43], that is

$$\boldsymbol{D}^{\mathrm{H}}=\frac{1}{|\Omega|}\int_{\Omega}\boldsymbol{D}_e\left(\boldsymbol{I}-\boldsymbol{b}\boldsymbol{\chi}\right)d\Omega \tag{1}$$

in which Ω and $|\Omega|$ represent the domain of micro unite cell and its area, respectively; $\boldsymbol{D}_e$ denotes the constitutive matrix of the e-th element; the symbol $\boldsymbol{I}$ stands for a unit matrix; The symbol $\boldsymbol{b}$ is the strain matrix at the micro-scale; $\boldsymbol{\chi}$ is the characteristic displacement of the microstructure.

The average mass density η^{H} of the micro unit cell can also be calculated based on the homogenization method as

$$\eta^{\mathrm{H}}=\frac{1}{|\Omega|}\int_{\Omega}\eta_e\mathrm{d}\Omega \tag{2}$$

Here, η_e is the mass density of the e-th element in the micro unit cell. The detailed derivations of the effective macro constitutive matrix $\boldsymbol{D}^{\mathrm{H}}$ and the average mass density η^{H} are provided in literature [6].

Considering the structural damping, the dynamic equilibrium equation of periodical composite structural-acoustic system can be derived as [12-13]

$$\begin{bmatrix}\boldsymbol{K}_s+i\omega\boldsymbol{C}_s-\omega^2\boldsymbol{M}_s & -\boldsymbol{H}\\ \rho_f\omega^2\boldsymbol{H}^{\mathrm{T}} & \boldsymbol{K}_f-\omega^2\boldsymbol{M}_f\end{bmatrix}\begin{Bmatrix}\boldsymbol{u}_s\\ \boldsymbol{p}\end{Bmatrix}=\begin{Bmatrix}\boldsymbol{F}_s\\ \boldsymbol{F}_f\end{Bmatrix} \tag{3}$$

Where $\boldsymbol{K}_s$ and $\boldsymbol{M}_s$ denote the stiffness matrix and mass matrix of the periodical composite structure; $\boldsymbol{C}_s$ is the structural damping matrix; $\boldsymbol{K}_f$ and $\boldsymbol{M}_f$ are the stiffness matrix and the mass matrix of the acoustic medium, respectively; $\boldsymbol{H}$ is the spatial coupled matrix between periodical composite structure and acoustic medium; $\boldsymbol{u}_s$ and $\boldsymbol{p}$ denote the displacement vector of periodical composite structural and sound pressure

vector in acoustic domain; $\boldsymbol{F}_s$ and $\boldsymbol{F}_f$ are the generalized force vectors related to the periodical composite plate and to the internal fluid cavity; ω is the angle frequency of external harmonic excitation; ρ_f is the density of the air.

To simplify the process of analyzing the dynamic equilibrium equation of the periodical composite structural-acoustic system, Eq. (3) can be rewritten as

$$\boldsymbol{Z}\boldsymbol{U} = \boldsymbol{F} \tag{4}$$

where $\boldsymbol{Z}$ represents the dynamic stiffness matrix of the periodical composite structural-acoustic system; $\boldsymbol{U}$ represents the dynamic frequency response vector; $\boldsymbol{F}$ is the external excitation vector. They can be expressed as

$$\boldsymbol{Z} = \begin{bmatrix} \boldsymbol{K}_s + i\omega\boldsymbol{C}_s - \omega^2\boldsymbol{M}_s & -\boldsymbol{H} \\ \rho_f\omega^2\boldsymbol{H}^{\mathrm{T}} & \boldsymbol{K}_f - \omega^2\boldsymbol{M}_f \end{bmatrix} \boldsymbol{U} = \begin{Bmatrix} \boldsymbol{u}_s & \boldsymbol{p} \end{Bmatrix}^{\mathrm{T}} \boldsymbol{F} = \begin{Bmatrix} \boldsymbol{F}_b & \boldsymbol{F}_q \end{Bmatrix}^{\mathrm{T}} \tag{5}$$

The effective macro constitutive matrix D^{H} and average mass density η^{H} obtained by the homogenization method are used to calculate the periodical composite structural stiffness matrix $\boldsymbol{K}_s$ and mass matrix $\boldsymbol{M}_s$, that is

$$\boldsymbol{K}_s = \sum_{j=1}^{N_{cell}} \left(\int_{\Omega_j} \boldsymbol{B}^{\mathrm{T}} \boldsymbol{D}^{\mathrm{H}} \boldsymbol{B} \mathrm{d}\Omega \right) \tag{6}$$

$$\boldsymbol{M}_s = \sum_{j=1}^{N_{cell}} \left(\int_{\Omega_j} \eta^{\mathrm{H}} \boldsymbol{N}_s^{\mathrm{T}} \boldsymbol{N}_s \mathrm{d}\Omega \right) \tag{7}$$

in which $\boldsymbol{N}_s$ represents the Lagrange shape function of the isoparametric quadrilateral element; $\boldsymbol{B}$ stands for the strain matrix of the macrostructure; Symbol N_{cell} and Symbol Ω_j denote the total number of discrete elements and the j-th element in the structural domain, respectively.

The Rayleigh damping model is used for the structural damping. The structural damping matrix $\boldsymbol{C}_s$ can be expressed as

$$\boldsymbol{C}_s = \alpha \boldsymbol{M}_s + \beta \boldsymbol{K}_s \tag{8}$$

where α and β are damping coefficients.

In the acoustic field, $\boldsymbol{K}_f$ and $\boldsymbol{M}_f$ can be expressed as

$$\boldsymbol{M}_f = \sum_{e=1}^{n_{cell}} \frac{1}{c^2} \int_{\Omega_e} \boldsymbol{N}_f^{\mathrm{T}} \boldsymbol{N}_f \mathrm{d}\Omega \tag{9}$$

$$\boldsymbol{K}_f = \sum_{e=1}^{n_{cell}} \int_{\Omega_e} (\nabla \boldsymbol{N}_f)^{\mathrm{T}} \cdot (\nabla \boldsymbol{N}_f) \mathrm{d}\Omega \tag{10}$$

where n_{cell} is the total number of elements in the acoustic field; Ω_e is the e-th element in the acoustic field; $\boldsymbol{N}_f$ is the Lagrange shape function of the isoparametric hexahedral element; c denotes the sound speed.

3. Definition of the bounded hybrid uncertain model

Multi-scale uncertainties exist simultaneously in the periodical composite structural-acoustic systems. At the micro-scale, the uncertainty may come from the constituent material properties of the microstructure due to manufacturing errors. The source of the uncertainties at the macro-scale is from the physical parameters of the acoustic medium and the external load resulting from the environment. In this paper, the bounded hybrid uncertain model is employed to describe the multi-scale uncertainties involved in periodical composite structural-acoustic system. In the bounded hybrid uncertain model, the interval variables are used to treat the uncertain-but-bounded parameters whose probabilistic information is missing, whereas the bounded random variables are used to deal with the uncertain-but-bounded parameters whose probability density functions are well defined. The multi-scale bounded hybrid uncertain vector can be expressed as

$\boldsymbol{x}=[\boldsymbol{x}^I,\boldsymbol{x}^R]=[x_1^I,x_2^I,...,x_{i_1}^I,x_{i_1+1}^R,...,x_{i_1+i_2}^R]$, in which $\boldsymbol{x}$ includes the interval vector and bounded random vector.

Assumed that $\boldsymbol{x}^I$ is an *n*-dimensional interval vector which includes all the interval variables $x_i^I(i=1,2,\ldots,n)$ in the periodical composite structural-acoustic system. The $\boldsymbol{x}^I$ can be expressed as

$$\begin{aligned}&\boldsymbol{x}\in\boldsymbol{x}^I=\left[\underline{\boldsymbol{x}}^I,\overline{\boldsymbol{x}}^I\right]=\left(x_i^I\right),\\&x_i\in x_i^I=\left[\underline{x}_i^I,\overline{x}_i^I\right],\ i=1,2,...,n\end{aligned}\tag{11}$$

where $\underline{\boldsymbol{x}}^I$ and $\overline{\boldsymbol{x}}^I$ are the lower and upper bounds of the interval vector; $\underline{x}_i^I$ and $\overline{x}_i^I$ are the lower and upper bounds of the *i*-th interval variable.

Assume that $\boldsymbol{x}^R$ is an *n*-dimensional bounded random vector which includes all the bounded random variables $x_i^R(i=1,2,\ldots,n)$ in the periodical composite structural-acoustic system. The $\boldsymbol{x}^R$ can be expressed as

$$\begin{aligned}&\boldsymbol{x}\in\boldsymbol{x}^R=\left[\underline{\boldsymbol{x}}^R,\overline{\boldsymbol{x}}^R\right]=\left(x_i^R\right),\\&x_i\in x_i^R=\left[\underline{x}_i^R,\overline{x}_i^R\right],\ i=1,2,...,n\end{aligned}\tag{12}$$

where $\underline{\boldsymbol{x}}^R$ and $\overline{\boldsymbol{x}}^R$ are the lower and upper bounds of the bounded random vector; $\underline{x}_i^R$ and $\overline{x}_i^R$ are the lower and upper bounds of the *i*-th bounded random variable.

4. HHSIPM for the hybrid interval and random analysis of the periodical composite structural-acoustic system with multi-scale bounded hybrid uncertain parameters

On the basis of the conventional first-order Taylor series expansion, a homogenization-based hybrid stochastic interval perturbation method (HHSIPM) is developed for the periodical composite structural-acoustic system with multi-scale bounded hybrid uncertain parameters. In the HHSIPM, the equivalent macroscopic

material properties are calculated through the homogenization method. Then, the matrix perturbation analysis based on the Taylor series expansion is performed for the periodical composite structural-acoustic system with multi-scale bounded hybrid uncertain parameters. The detailed process of the matrix perturbation analysis has been introduced in literature [44]. It should be noticed here that the expectation and the variance of the bounded random variable can be obtained by tremendous sampling according to the statistical data of the bounded random variable.

Considering the interval vector as a constant, the dynamic stiffness matrix $\boldsymbol{Z}(\boldsymbol{x}^I, \boldsymbol{x}^R)$ and the external excitation vector $\boldsymbol{F}(\boldsymbol{x}^I, \boldsymbol{x}^R)$ can be approximated by the first-order Taylor expansion at the expectation of the bounded random vector $\boldsymbol{x}^R$.

Based on the perturbation theory, Eq. (4) can be transformed into

$$\boldsymbol{U}(\boldsymbol{x}^I, \boldsymbol{x}^R) = \left(\boldsymbol{Z}^m + \Delta\boldsymbol{Z}\right)^{-1}\left(\boldsymbol{F}^m + \Delta\boldsymbol{F}\right) \tag{13}$$

Where, $\boldsymbol{Z}^m$ and $\boldsymbol{F}^m$ represent the mean value of the dynamic stiffness matrix and the external excitation vector, respectively; $\Delta\boldsymbol{Z}$ and $\Delta\boldsymbol{F}$ are the deviations of the dynamic stiffness matrix and the external excitation vector. The detailed derivations of the mean value and deviations are given in reference [44].

The $\left(\boldsymbol{Z}^m + \Delta\boldsymbol{Z}\right)^{-1}$ can be approximated by Neumann series expansion when the spectral radius of $\left(\boldsymbol{Z}^m\right)^{-1}\Delta\boldsymbol{Z}$ is less than 1 [45]. By neglecting the higher order terms of Neumann series, the sound pressure vector $\boldsymbol{U}(\boldsymbol{x}^I, \boldsymbol{x}^R)$ can be rewritten as following

$$\begin{aligned}\boldsymbol{U}(\boldsymbol{x}^I, \boldsymbol{x}^R) = &\left(\boldsymbol{Z}^m\right)^{-1}\boldsymbol{F}^m + \left(\boldsymbol{Z}^m\right)^{-1}\sum_i^{L_1}\frac{\boldsymbol{F}(\mu(\boldsymbol{x}^R), \boldsymbol{x}^I)}{\partial x_i^R}\left(x_i^R - \mu(x_i^R)\right) \\ &-\left(\boldsymbol{Z}^m\right)^{-1}\sum_i^{L_1}\frac{\boldsymbol{Z}(\mu(\boldsymbol{x}^R), \boldsymbol{x}^I)}{\partial x_i^R}\left(x_i^R - \mu(x_i^R)\right)\left(\boldsymbol{Z}^m\right)^{-1}\boldsymbol{F}^m\end{aligned} \tag{14}$$

In the above equation, L_1 represents the total number of the bounded random variables; $\mu(\boldsymbol{x}^R)$ and $\mu(x_i^R)$ are the expectations of the bounded random vector and i-th bounded random variable, respectively; The detailed derivations of the first derivative of $\boldsymbol{Z}(\boldsymbol{x}^I, \boldsymbol{x}^R)$ and $\boldsymbol{F}(\boldsymbol{x}^I, \boldsymbol{x}^R)$ can be found in references [6,11].

Based on the random moment method, in which the expectation and variance are respectively the first-order raw moment and second central moment, the expectation and variance of sound response of the periodical composite structural-acoustic system can be expressed as

$$E(\boldsymbol{x}^I) = \mu\left(\boldsymbol{U}(\boldsymbol{x}^I, \boldsymbol{x}^R)\right) = \left(\boldsymbol{Z}(\mu(\boldsymbol{x}^R), \boldsymbol{x}_m^I))\right)^{-1} \boldsymbol{F}(\mu(\boldsymbol{x}^R), \boldsymbol{x}_m^I) \tag{15}$$

$$\begin{aligned} S(\boldsymbol{x}^I) &= \sigma^2\left(\boldsymbol{U}(\boldsymbol{x}^I, \boldsymbol{x}^R)\right) \\ &= \sum_{i_1}^{L_1}\sum_{i_2}^{L_1}\left(\left(\boldsymbol{Z}^m\right)^{-1}\frac{\boldsymbol{F}(\mu(\boldsymbol{x}^R), \boldsymbol{x}^I)}{\partial x_{i_1}^R} - \left(\boldsymbol{Z}^m\right)^{-1}\frac{\boldsymbol{Z}(\mu(\boldsymbol{x}^R), \boldsymbol{x}^I)}{\partial x_{i_1}^R}\left(\boldsymbol{Z}^m\right)^{-1}\boldsymbol{F}^m\right) \\ &\times\left(\left(\boldsymbol{Z}^m\right)^{-1}\frac{\boldsymbol{F}(\mu(\boldsymbol{x}^R), \boldsymbol{x}^I)}{\partial x_{i_2}^R} - \left(\boldsymbol{Z}^m\right)^{-1}\frac{\boldsymbol{Z}(\mu(\boldsymbol{x}^R), \boldsymbol{x}^I)}{\partial x_{i_2}^R}\left(\boldsymbol{Z}^m\right)^{-1}\boldsymbol{F}^m\right) \\ &\times cov(x_{i_2}^R, x_{i_2}^R) \end{aligned} \tag{16}$$

where $\boldsymbol{x}_m^I$ represents the mean value of interval vector $\boldsymbol{x}^I$.

Considering that the expectation and the variance of the sound response are interval vectors, the bounds of expectation and variance can be obtained through the interval analysis method [44]. The bounds of the expectation of the sound response are given by

$$\begin{aligned} E\left(\boldsymbol{U}(\boldsymbol{x}^I, \boldsymbol{x}^R)\right)_{lower} &= E^m - \Delta E \\ E\left(\boldsymbol{U}(\boldsymbol{x}^I, \boldsymbol{x}^R)\right)_{upper} &= E^m + \Delta E \end{aligned} \tag{17}$$

where E^m and ΔE can be expressed as

$$E^m = \left(\boldsymbol{Z}^m\right)^{-1}\boldsymbol{F}^m \tag{18}$$

$$\Delta E = \left|\sum_{j}^{L_2}\frac{\left(\boldsymbol{Z}_{upper}\right)^{-1}\boldsymbol{F}_{upper} - \left(\boldsymbol{Z}_{lower}\right)^{-1}\boldsymbol{F}_{lower}}{2}\right| \tag{19}$$

In the above equation, L_2 represents the total number of the interval variables; The detail expression of $\boldsymbol{Z}_{upper}$, $\boldsymbol{Z}_{lower}$, $\boldsymbol{F}_{upper}$, $\boldsymbol{F}_{lower}$ can be deduced according to the literature [44].

Similarly, the bounds of the variance of sound response are expressed as

$$\begin{aligned} S\left(\boldsymbol{U}(\boldsymbol{x}^I,\boldsymbol{x}^R)\right)_{lower} &= S^m - \Delta S \\ S\left(\boldsymbol{U}(\boldsymbol{x}^I,\boldsymbol{x}^R)\right)_{upper} &= S^m + \Delta S \end{aligned} \tag{20}$$

where S^m and ΔS are determined by

$$\begin{aligned} S^m = \sum_{i_1}^{L_1}\sum_{i_2}^{L_1}\Bigg(&\left(\boldsymbol{Z}^m\right)^{-1}\frac{\partial \boldsymbol{F}^m}{\partial x_{i_1}^R} - \left(\boldsymbol{Z}^m\right)^{-1}\frac{\partial \boldsymbol{Z}^m}{\partial x_{i_1}^R}\left(\boldsymbol{Z}^m\right)^{-1}\boldsymbol{F}^m\Bigg) \\ &\times\left(\left(\boldsymbol{Z}^m\right)^{-1}\frac{\partial \boldsymbol{F}^m}{\partial x_{i_2}^R} - \left(\boldsymbol{Z}^m\right)^{-1}\frac{\partial \boldsymbol{Z}^m}{\partial x_{i_2}^R}\left(\boldsymbol{Z}^m\right)^{-1}\boldsymbol{F}^m\right) \\ &\times cov(x_{i_1}^R, x_{i_2}^R) \end{aligned} \tag{21}$$

$$\begin{aligned} \Delta S = \frac{1}{2}\Bigg|\sum_{j}^{L_2}\Bigg(&\sum_{i_1}^{L_1}\sum_{i_2}^{L_1}\Bigg(\left(\boldsymbol{Z}_{upper}\right)^{-1}\frac{\partial \boldsymbol{F}_{upper}}{\partial x_{i_1}^R} - \left(\boldsymbol{Z}_{upper}\right)^{-1}\frac{\partial \boldsymbol{Z}_{upper}}{\partial x_{i_1}^R}\left(\boldsymbol{Z}_{upper}\right)^{-1}\boldsymbol{F}_{upper}\Bigg) \\ &\times\left(\left(\boldsymbol{Z}_{upper}\right)^{-1}\frac{\partial \boldsymbol{F}_{upper}}{\partial x_{i_2}^R} - \left(\boldsymbol{Z}_{upper}\right)^{-1}\frac{\partial \boldsymbol{Z}_{upper}}{\partial x_{i_2}^R}\left(\boldsymbol{Z}_{upper}\right)^{-1}\boldsymbol{F}_{upper}\right)cov(x_{i_1}^R, x_{i_2}^R) \\ &-\sum_{i_1}^{L_1}\sum_{i_2}^{L_1}\Bigg(\left(\boldsymbol{Z}_{lower}\right)^{-1}\frac{\partial \boldsymbol{F}_{lower}}{\partial x_{i_1}^R} - \left(\boldsymbol{Z}_{lower}\right)^{-1}\frac{\partial \boldsymbol{Z}_{lower}}{\partial x_{i_1}^R}\left(\boldsymbol{Z}_{lower}\right)^{-1}\boldsymbol{F}_{lower}\Bigg) \\ &\times\left(\left(\boldsymbol{Z}_{lower}\right)^{-1}\frac{\partial \boldsymbol{F}_{lower}}{\partial x_{i_2}^R} - \left(\boldsymbol{Z}_{lower}\right)^{-1}\frac{\partial \boldsymbol{Z}_{lower}}{\partial x_{i_2}^R}\left(\boldsymbol{Z}_{lower}\right)^{-1}\boldsymbol{F}_{lower}\right)cov(x_{i_1}^R, x_{i_2}^R)\Bigg)\Bigg| \end{aligned} \tag{22}$$

5. HGPEM for the hybrid interval and random analysis of the periodical composite structural-acoustic system with multi-scale bounded hybrid uncertain parameters

Considering that the orthogonal polynomial approximation method is free of the derivative process and not limited on uncertain problems with small uncertain level, the Gegenbauer polynomial expansion is introduced for the hybrid interval and random analysis of periodical composite structural-acoustic systems with multi-scale uncertainties to obtain a better accuracy compared with the HHSIPM. Owing to the use of λ-PDF model in HGPEM, we mainly focus on the application of HGPEM to solve uncertain problem with mono-peak or mono-valley PDFs.

5.1. The theory of Gegenbauer polynomial expansion

The general expressions for Gegenbauer polynomials of *n* degree denoted by $G_n^{\lambda}(\xi)$ can be expressed as [46]

$$G_n^{\lambda}(\xi)=\sum_{k=0}^{n}\frac{1}{k!(n-k)!}\frac{(2\lambda)_n(2\lambda+n)_k}{(\lambda+1/2)_k}(\frac{\xi-1}{2})^k \quad n=0,1,2,... \tag{23}$$

where λ is the polynomial parameter that satisfies λ>0; Pochhammer symbol $(\lambda)_k$ is used for conciseness:

$$(\lambda)_k=\lambda(\lambda+1)\cdots(\lambda+k-1)=\frac{\Gamma(\lambda+k)}{\Gamma(\lambda)} \tag{24}$$

in which $\Gamma(\bullet)$ is the Gamma function and $(\lambda)_0 \equiv 1$.

Another significant property of standard Gegenbauer polynomials is defined by the recurrence relation as follow:

$$
\begin{aligned}
&G_0^{\lambda}(\xi)=1\\
&G_1^{\lambda}(\xi)=2\lambda\xi\\
&\cdots\\
&(n+1)G_{n+1}^{\lambda}(\xi)=2(n+\lambda)\xi G_n^{\lambda}(\xi)-(n+2\lambda-1)G_{n-1}^{\lambda}(\xi)\quad n\geq 2
\end{aligned}
\tag{25}
$$

The orthogonal relationships of Gengenbaur polynomials on $\xi\in[-1,1]$ can be expressed as

$$
\int_{-1}^{1}\rho_{\lambda}(\xi)G_m^{\lambda}(\xi)G_n^{\lambda}(\xi)d\xi=\begin{cases}b_n^{\lambda} & m=n\\ 0 & m\neq n\end{cases}
\tag{26}
$$

where weight function $\rho_{\lambda}(\xi)$ and b_n^{λ} can be expressed as

$$
\rho_{\lambda}(\xi)=a_{\lambda}\left(1-\xi^2\right)^{\lambda-\frac{1}{2}},\quad a_{\lambda}=\frac{\Gamma\left(\lambda+1\right)}{\Gamma\left(1/2\right)\Gamma\left(\lambda+1/2\right)}
\tag{27}
$$

$$
b_n^{\lambda}=\frac{\Gamma(1/2)}{2^{2\lambda-1}n!}\cdot\frac{\lambda\Gamma(2\lambda+n)}{(\lambda+n)\Gamma\left(\lambda\right)\Gamma(\lambda+1/2)}
\tag{28}
$$

L-dimensional continuous function $f(\boldsymbol{\xi})$ ($\boldsymbol{\xi}=[\xi_1,\xi_2,\cdots,\xi_l,\cdots\xi_L]$) defined on $\xi_l\in[-1,1]$ can be approximated as the N_l-order Gegenbauer polynomials owing to the orthogonal relationships of Gegenbauer polynomials [18], that is

$$
f(\boldsymbol{\xi})\approx\sum_{i_1=0}^{N_1}\cdots\sum_{i_L=0}^{N_L}g_{i_1i_2\cdots i_L}G_{i_1,\ldots,i_L}^{\lambda_1,\ldots,\lambda_L}(\boldsymbol{\xi})
\tag{29}
$$

Where $g_{i_1i_2\cdots i_L}$ is the expansion coefficient to be estimated; $G_{i_1,\ldots,i_L}^{\lambda_1,\ldots,\lambda_L}(\boldsymbol{\xi})$ denotes the L-dimensional Gegenbauer polynomials which can be expressed as $G_{i_1,\ldots,i_L}^{\lambda_1,\ldots,\lambda_L}(\boldsymbol{\xi})=G_{i_1}^{\lambda_1}(\xi_1)G_{i_2}^{\lambda_2}(\xi_2)\cdots G_{i_L}^{\lambda_L}(\xi_L)$. $N_l(l=1,2,\ldots,L)$ are the retained orders the of Gegenbauer polynomials related to ξ_l.

To avoid the shortcoming of Galerkin technique that the dimension of the transformed equations exceeds the degrees of freedom of the periodical composite structural-acoustic system, the weighted least squares method and the Gauss-Gegenbauer integration formula are adopted to compute the expansion

coefficient $g_{i_1\cdots i_L}$ of Gegenbauer polynomials [47], that is

$$g_{i_1\cdots i_L} \approx \frac{1}{b_1^{\lambda_1}\times\cdots\times b_L^{\lambda_L}}\sum_{j_1=1}^{m_1}\cdots\sum_{j_L=1}^{m_L} f(\hat{\xi}_{j_1}^{\lambda_1},\cdots,\hat{\xi}_{j_L}^{\lambda_L}) \times G_{i_1,\ldots,i_L}^{\lambda_1,\ldots,\lambda_L}(\hat{\xi}_{j_1}^{\lambda_1},\ldots,\hat{\xi}_{j_L}^{\lambda_L})A_{j_1}^{\lambda_1}A_{j_2}^{\lambda_2}\cdots A_{j_L}^{\lambda_L} \tag{30}$$

In the above equation, $m_l (l=1,2,\ldots,L)$ represent the total number of the interpolation points $\hat{\xi}_{j_l}^{\lambda_l}(l=1,2,\ldots,L)$ of Gauss-Gegenbauer integration and $m_i = N_i + 1$. The interpolation points are the roots of $G_{m_l}^{\lambda_l}(\xi)$. The weight $A_{j_l}^{\lambda_l}$ are expressed as [47]

$$A_{j_l}^{\lambda_l} = 2^{2-2\lambda_l}\pi\left\{\Gamma(\lambda_l)\right\}^{-2}\frac{\Gamma(m_l+2\lambda_l)}{\Gamma(m_l+1)} \times\left\{1-\left(\hat{\xi}_{j_l}^{\lambda_l}\right)^2\right\}^{-1}\left\{2\lambda_l G_{m_l-1}^{\lambda_l+1}(\hat{\xi}_{j_l}^{\lambda_l})\right\}^{-2} \tag{31}$$

5.2. Transformation of bounded random variables and interval variables

In order to approximate the response of periodical composite structural-acoustic system with arbitrary interval vector $\boldsymbol{x}^I$ through the Gengenbauer polynomials defined on $\xi\in[-1,1]$, the interval variables x_i^I should be transformed to the linear function of the unitary interval variables $\xi_i^I \in [-1,1]$ [18], that is

$$\begin{aligned}&\boldsymbol{x}^I = \boldsymbol{\psi}^I(\boldsymbol{\xi}^I), \boldsymbol{\xi}^I = [\xi_1^I,\xi_2^I,\ldots,\xi_L^I],\\ &x_i^I = \psi_i^I(\xi_i^I) = \frac{\underline{x}_i^I + \overline{x}_i^I}{2} + \frac{\underline{x}_i^I - \overline{x}_i^I}{2}\xi_i^I,\ i=1,2,\ldots,L\end{aligned} \tag{32}$$

Here, $\psi_i^I(\xi_i^I)$ denotes the interval transformation function with respect to the unitary interval variable ξ_i^I.

Similarly, the arbitrary bounded random variables x_i^R should be transformed to a function of the unitary bounded random variables $\xi_i^R \in [-1,1]$, that is

$$\begin{aligned}&\boldsymbol{x}^R = \boldsymbol{\psi}^R(\boldsymbol{\xi}^R), \boldsymbol{\xi}^R = [\xi_1^R,\xi_2^R,\ldots,\xi_L^R],,\\ &x_i^R = \psi_i^R(\xi_i^R) = c_{i,0} + c_{i,1}\xi_i^R + c_{i,2}\left(\xi_i^R\right)^2 + \cdots,\ i=1,2,\ldots,L\end{aligned} \tag{33}$$

in which, $\psi_i^R(\xi_i^R)$ denotes the bounded random transformation function with respect to the unitary bounded random variable ξ_i^R. $c_{i,0}, c_{i,1}, c_{i,2}\cdots$ are the transformation coefficients of the bounded random transformation function $\psi_i^R(\xi_i^R)$.

The truncated PDF of bounded random variables are defined as

$$P(x_i^R) = \begin{cases} \geq 0 & x_i^R \in \left[\underline{x}_i^R, \overline{x}_i^R\right] \\ = 0 & x_i^R \notin \left[\underline{x}_i^R, \overline{x}_i^R\right] \end{cases} \tag{34}$$

The random analysis for composite structural-acoustic system is on the basis that using the Gegenbauer polynomials to represent bounded random variables. Gegenbauer polynomial is a parametric polynomial, hence it can be applied to represent a series of truncated PDFs that is λ-PDF. The λ-PDF of unitary bounded random variables ξ_i^R can be defined as

$$P_{\lambda^R}(\xi_i^R) = \rho_{\lambda^R}(\xi_i^R) = \begin{cases} a_{\lambda^R}\left(1-\left(\xi_i^R\right)^2\right)^{\lambda^R-\frac{1}{2}} & \xi_i^R \in [-1,1] \\ 0 & \xi_i^R \notin [-1,1] \end{cases} \tag{35}$$

Where, $\rho_\lambda(\xi_i^R)$ is the weight function of Gegenbauer polynomial as show in Eq. (27); λ^R is the polynomial parameter for bounded random variables.

The polynomial parameter λ^R and transformation coefficients $c_{i,0}, c_{i,1}, c_{i,2}\cdots$ can be calculated through the optimization method as follows [48]

$$\begin{aligned} &\text{To find } \lambda^R, c_{i,k}\,(k=0,1,...) \\ &\text{Min} \quad \sum_{i=1}^{N}\left[P_{ori}(x_i^R) - P_{\lambda^R}(x_i^R)\right]^2 \end{aligned} \tag{36}$$

here, $P_{ori}(x_i^R)$ is the original PDF of the bounded random variable x_i^R, and $P_{\lambda^R}(x_i^R)$ is the PDF of the polynomial function $\boldsymbol{\psi}^R(\xi_i^R)$.

We can find from Eq. (32) that the polynomial parameter λ^I for the interval

variables is independent with transformation function. Theoretically, λ^I can take any value that satisfies $\lambda^I > 0$. However, the accuracy of Gegenbauer polynomials depends upon the choice of λ^I. Literature [18] has discussed how to find the optimal value of λ^I through a simple function. Conclusion has been drawn that the accuracy of Gegenbauer polynomials with respect to interval variables can be improved through decreasing the value of λ^I.

5.3. The bounds of expectation and variance of the sound response in the periodical structural-acoustic system with multi-scale bounded hybrid uncertain parameters

The response of the periodical composite structural-acoustic system with multi-scale bounded hybrid uncertain parameters is a hybrid function with respect to the interval variables and the bounded random variables. According to the Eq. (29), the sound response vector $\boldsymbol{U}(\boldsymbol{x}^I, \boldsymbol{x}^R)$ can be approximated by Gegenbauer polynomials as

$$\begin{aligned} \boldsymbol{U}(\boldsymbol{x}^I, \boldsymbol{x}^R) &= \boldsymbol{U}\left(\boldsymbol{\psi}^I(\boldsymbol{\xi}^I), \boldsymbol{\psi}^R(\boldsymbol{\xi}^R)\right) \\ &= \sum_{i_1=0}^{N_1} \cdots \sum_{i_L=0}^{N_L} g_{i_1,\cdots,i_L} G_{i_1,\cdots,i_{L_1}}^{\lambda_1^I,\cdots,\lambda_{L_1}^I}(\boldsymbol{\xi}^I) G_{i_{L_1+1},\cdots,i_L}^{\lambda_{L_1+1}^R,\cdots,\lambda_L^R}(\boldsymbol{\xi}^R) \end{aligned} \tag{37}$$

in which the interval transformation function vector $\boldsymbol{\psi}^I = [\psi_1^I, \psi_2^I, ..., \psi_{L_1}^I]$ is determined by Eq. (32), and the polynomial parameter $\lambda_i^I (i = 1, 2, ..., L_1)$ for interval variable are all taken as very small values; The bounded random transformation function vector $\boldsymbol{\psi}^R = [\psi_{L_1+1}^R, \psi_{L_1+2}^R, ..., \psi_L^R]$ and the polynomial parameter $\lambda_i^R (i = L_1 + 1, L_1 + 2, ..., L)$ for the bounded random variable are determined by Eqs. (33) and (36), respectively; $\hat{\boldsymbol{\xi}}^{\lambda^I}$ and $\hat{\boldsymbol{\xi}}^{\lambda^R}$ are Gaussian interpolation points for interval variables and bounded random variables, respectively; The sound response

vector at Gaussian interpolation points $\hat{\boldsymbol{\xi}}^{\lambda^I}$ and $\hat{\boldsymbol{\xi}}^{\lambda^R}$ is calculated by

$$\boldsymbol{U}\left(\boldsymbol{\psi}^I(\hat{\boldsymbol{\xi}}^{\lambda^I}),\boldsymbol{\psi}^R(\hat{\boldsymbol{\xi}}^{\lambda^R})\right)=\boldsymbol{Z}^{-1}\left(\boldsymbol{\psi}^I(\hat{\boldsymbol{\xi}}^{\lambda^I}),\boldsymbol{\psi}^R(\hat{\boldsymbol{\xi}}^{\lambda^R})\right)\boldsymbol{F}\left(\boldsymbol{\psi}^I(\hat{\boldsymbol{\xi}}^{\lambda^I}),\boldsymbol{\psi}^R(\hat{\boldsymbol{\xi}}^{\lambda^R})\right) \tag{38}$$

The stiffness matrix and mass matrix of the periodical composite structure at interpolation points of Gaussian integration can be computed by

$$\boldsymbol{K}_s\left(\boldsymbol{\psi}^I(\hat{\boldsymbol{\xi}}^{\lambda^I}),\boldsymbol{\psi}^R(\hat{\boldsymbol{\xi}}^{\lambda^R})\right)=\sum_{j=1}^{N_{cell}}\left(\int_{\Omega_j}\boldsymbol{B}^{\mathrm{T}}\boldsymbol{D}^{\mathrm{H}}\left(\boldsymbol{\psi}^I(\hat{\boldsymbol{\xi}}^{\lambda^I}),\boldsymbol{\psi}^R(\hat{\boldsymbol{\xi}}^{\lambda^R})\right)\boldsymbol{B}\mathrm{d}\Omega\right) \tag{39}$$

$$\boldsymbol{M}_s\left(\boldsymbol{\psi}^I(\hat{\boldsymbol{\xi}}^{\lambda^I}),\boldsymbol{\psi}^R(\hat{\boldsymbol{\xi}}^{\lambda^R})\right)=\sum_{j=1}^{N_{cell}}\left(\int_{\Omega_j}\eta^{\mathrm{H}}\left(\boldsymbol{\psi}^I(\hat{\boldsymbol{\xi}}^{\lambda^I}),\boldsymbol{\psi}^R(\hat{\boldsymbol{\xi}}^{\lambda^R})\right)\boldsymbol{N}_s^{\mathrm{T}}\boldsymbol{N}_s\mathrm{d}\Omega\right) \tag{40}$$

The sound response of the *r*-th element is expressed as

$$\begin{aligned}U_r(\boldsymbol{x}^I,\boldsymbol{x}^R)&=U_r\left(\boldsymbol{\psi}^I(\boldsymbol{\xi}^I),\boldsymbol{\psi}^R(\boldsymbol{\xi}^R)\right)\\&=\sum_{i_1=0}^{N_1}\cdots\sum_{i_L=0}^{N_L}g^r_{i_1,\cdots,i_L}\times G^{\lambda_1^I,\cdots,\lambda_{L_1}^I}_{i_1,\cdots,i_{L_1}}(\boldsymbol{\xi}^I)G^{\lambda_{L_1+1}^R,\cdots,\lambda_L^R}_{i_{L_1+1},\cdots,i_L}(\boldsymbol{\xi}^R)\quad r=1,2,...,N\end{aligned} \tag{41}$$

where the expansion coefficient $g^r_{i_1,\cdots,i_L}$ of *r*-th element can be written as

$$\begin{aligned}g^r_{i_1,\cdots,i_L}\approx&\frac{1}{b_1^{\lambda_1}\times\cdots b_L^{\lambda_L}}\sum_{j_1=1}^{m_1}\cdots\sum_{j_L=1}^{m_L}U_r\left(\boldsymbol{\psi}^I(\hat{\boldsymbol{\xi}}^{\lambda^I}),\boldsymbol{\psi}^R(\hat{\boldsymbol{\xi}}^{\lambda^R})\right)\\&\times G^{\lambda_1,\cdots,\lambda_{L_1}}_{i_1,\cdots,i_{L_1}}(\hat{\boldsymbol{\xi}}^{\lambda^I})G^{\lambda_{L_1+1},\cdots,\lambda_L}_{i_{L_1+1},\cdots,i_L}(\hat{\boldsymbol{\xi}}^{\lambda^R})A^{\lambda^I}A^{\lambda^R}\end{aligned} \tag{42}$$

In the above equation, A^{λ^I} and A^{λ^R} are the weights for interval vector and bounded random vector;

On the basis of the Gegenbauer polynomials expansion, the expectation and variance of the sound pressure $U_r(x^I,x^R)$ of the periodical composite structural-acoustic system with multi-scale bounded hybrid parameters can be calculated by [18,48]

$$\begin{aligned}\mu_{U_r}&=\mu_{U_r}(\boldsymbol{\xi}^I)=E\left[U_r(\boldsymbol{x}^I,\boldsymbol{x}^R)\right]\\&=\sum_{i_1=0}^{N_1}\cdots\sum_{i_{L_1}=0}^{N_{L_1}}g^r_{i_1,\ldots,i_{L_1},0,\ldots,0}\times G^{\lambda_1^I,\cdots,\lambda_{L_1}^I}_{i_1,\cdots,i_{L_1}}(\boldsymbol{\xi}^I)\end{aligned} \tag{43}$$

$$\begin{aligned}\sigma_{U_r}^2 &= \sigma_{U_r}^2(\boldsymbol{\xi}^I) = E\left[\left(U_r(\boldsymbol{x}^I,\boldsymbol{x}^R)\right)^2\right] - \left(\mu_{U_r}\right)^2 \\ &= \sum_{i_{L_1+1}=0}^{N_{L_1+1}} \cdots \sum_{i_L=0}^{N_L} \left(\sum_{i_1=0}^{N_1} \cdots \sum_{i_{L_1}=0}^{N_{L_1}} g^r_{i_1,\ldots,i_L} \times G^{\lambda_1^I,\cdots,\lambda_{L_1}^I}_{i_1,\cdots,i_{L_1}}(\boldsymbol{\xi}^I) \right)^2 b^{\lambda_{L_1+1}}_{i_{L_1+1}} \cdots b^{\lambda_L}_{i_L} \\ &\quad - \left(\sum_{i_1=0}^{N_1} \cdots \sum_{i_{L_1}=0}^{N_{L_1}} g^r_{i_1,\ldots,i_{L_1},0,\ldots,0} \times G^{\lambda_1^I,\cdots,\lambda_{L_1}^I}_{i_1,\cdots,i_{L_1}}(\boldsymbol{\xi}^I) \right)^2\end{aligned} \tag{44}$$

It can be seen from Eqs. (43) and (44) that the expectation and variance of the sound response are polynomials functions with respect to unitary interval vector $\boldsymbol{\xi}^I$. For a relatively simple function with interval parameters, the scanning method is a suitable way to compute the precise bounds and its computational cost is very small. Thus, the lower and upper bounds of the expectation and variance can be obtained by scanning method and expressed as

$$\left(\mu_{U_r}\right)_{lower} = \min_{i=1,2,\ldots,M}\left\{\mu_{U_r}(\boldsymbol{\xi}^I)\right\}, \left(\mu_{U_r}\right)_{upper} = \max_{i=1,2,\ldots,M}\left\{\mu_{U_r}(\boldsymbol{\xi}^I)\right\} \tag{45}$$

$$\left(\sigma^2_{U_r}\right)_{lower} = \min_{i=1,2,\ldots,M}\left\{\sigma^2_{U_r}(\boldsymbol{\xi}^I)\right\}, \left(\sigma^2_{U_r}\right)_{upper} = \max_{i=1,2,\ldots,M}\left\{\sigma^2_{U_r}(\boldsymbol{\xi}^I)\right\} \tag{46}$$

where *M* represents the total number of sampling with the scanning method.

5.4. The procedure of the proposed HGPEM

In this section, a HGPEM for the periodical composite structural-acoustic system with multi-scale bounded hybrid uncertain parameters is developed by incorporating the Gegenbauer polynomial expansion into the HFEM. The procedure of the HGPEM can be summarized as follows

(1) Carrying out the homogenization analysis on the microstructure to obtain the effective macro constitutive matrix D^{H} and the average mass density η^{H} according to Eqs. (1) and (2);

(2) Carrying out the finite element analysis on the periodical composite structure

to calculate the stiffness matrix $\boldsymbol{K}_s$ and mass matrix $\boldsymbol{M}_s$ of the periodical composite structure using the effective macro constitutive matrix D^{H} and the average mass density η^{H} according to Eqs. (6) and (7);

(3) Carrying out the finite element analysis on the acoustic medium to compute the acoustic stiffness matrix $\boldsymbol{K}_f$ and the acoustic mass matrix $\boldsymbol{M}_f$ at macro-scale according to Eqs. (9) and (10);

(4) Generating the interpolation points of Gauss-Gegenbauer integration and calculating the weights of Gegenbauer polynomials for the interval vector and bounded random vector at the interpolation points according to Eq. (31);

(5) Calculating the sound response amplitude of the periodical composite structural-acoustic system at the interpolation points based on the HFEM;

(6) Calculating the expansion coefficients by using the Gauss-Gegenbauer integration method according to Eq. (42);

(7) Calculating the expectation and variance of sound response amplitude of the periodical composite structural-acoustic system with multi-scale bounded hybrid uncertain parameters on the basis of the Gegenbauer polynomials expansion according to Eqs. (43) and (44), respectively;

(8) Calculating the lower and upper bounds of the expectation and variance of the sound pressure amplitude through Eqs. (45) and (46).

6. Numerical example and analysis

6.1. A hexahedral box

Fig. 1 shows a three-dimensional cavity enclosed with a hexahedral box of

dimensions 0.25m × 0.25m ×0.25 m. A thin plate composed of periodic uniform unidirectional fiber reinforced composites is clamped at the top surface of the hexahedral box. Excepting the plate structure, the other surfaces of the box are rigid. The plate is excited by a concentrated harmonic loading F=10 N at its middle point. The clamped plate is discretized by 64 four-node Kirchhoff plate elements and the acoustic medium is discretized by 512 hexahedral elements. The point A is used to observe the sound pressure amplitude in the acoustic domain.

The unit Representative Volume Element (RVE) of the unidirectional fiber reinforced composites is shown in Fig. 2. For simplicity, the unit cells at the micro-scale are considered to be squared with dimensionless length of 1 × 1. The radius of the fiber at the center of the matrix is 0.2. The microstructure unit cell contains two prescribed materials, which are the strong material (red color) and the soft material (green color). The finite element model of the RVE is composed of 361 nodes and 340 quadrangle elements.

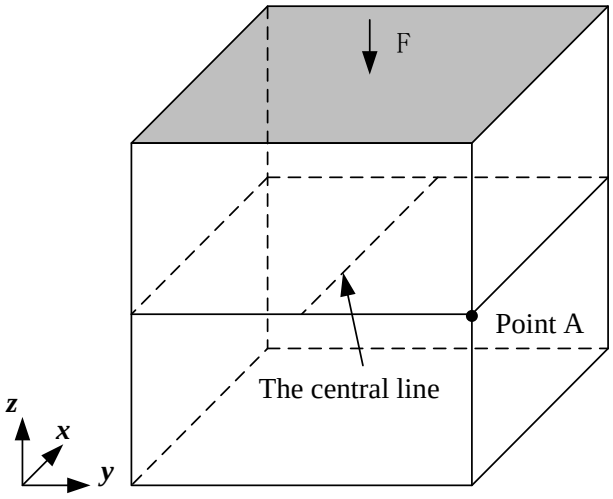

Fig. 1 A hexahedral box

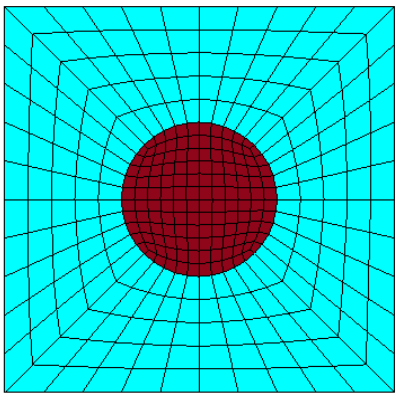

Fig. 2 RVE of a unidirectional fiber reinforced composites

The thickness of the periodical composite plate is t=1mm. The damping coefficients of the periodical composite plate are α=0.1 and β=0.5. The Poisson's ratios of the strong material and the soft material are v_1=v_2=0.3. The Young's modulus and mass density of the strong material are E_1=210 GPa and ρ_1=7800 kg/m^3, respectively. The Young's modulus and mass density of the soft material are E_2=21 GPa and ρ_2=780 kg/m^3, respectively. The density and the sound speed of the air are ρ_f=1.21 kg/m^3 and c=340.5 m/s, respectively.

To consider the uncertainty in the material properties of the microstructure unit cell, the Young's modulus and mass density of the fiber and the matrix are assumed to be independent bounded random variables. α_R denotes the uncertain level of these bounded random variables. The variation ranges of the bounded random variables can be expressed as

$$\begin{aligned} &E_1^R = E_1\left[1-\alpha_R,\ 1+\alpha_R\right], E_2^R = E_2\left[1-\alpha_R,\ 1+\alpha_R\right] \\ &\rho_1^R = \rho_1\left[1-\alpha_R,\ 1+\alpha_R\right], \rho_2^R = \rho_2\left[1-\alpha_R,\ 1+\alpha_R\right] \end{aligned} \tag{47}$$

Based on the transformation process of general bounded random variables in Section 5.2, the original PDF of the general bounded random variable can be approximated as a function of ξ^R. All of the original PDFs of the bounded random

variables are supposed to be linear functions of ξ^R for brevity but without loss of generality, that are

$$\begin{aligned} P_{\lambda_1}(E_1^R) &= E_1 + P_{\lambda_1}(\xi_{\lambda_1}^R)\triangle E_1,\ P_{\lambda_2}(E_2^R) = E_2 + P_{\lambda_2}(\xi_{\lambda_2}^R)\triangle E_2 \\ P_{\lambda_3}(\rho_1^R) &= \rho_1 + P_{\lambda_3}(\xi_{\lambda_3}^R)\triangle \rho_1, P_{\lambda_4}(\rho_2^R) = \rho_2 + P_{\lambda_4}(\xi_{\lambda_4}^R)\triangle \rho_2 \end{aligned} \tag{48}$$

Taking the Young's modulus of the strong material as an example, the original probabilistic distribution of the bounded random variable E_1^R is assumed to be a transformation of the Beta distribution and the uncertain level α_R is set as 0.2. According to the probabilistic distribution and α_R, the original statistical data of E_1^R is plotted in Figure 3 by using MATLAB. Based on the optimization process as shown in Eq. (36), the original PDF of E_1^R is approximated by a function of λ-PDF with λ^R =4, $c_{i,0} = 210$ and $c_{i,0} = 42$. The approximated PDF is also plotted in Figure 3. By tremendous sampling according to the original statistical data of E_1^R, the expectation and the variance of E_1^R can be obtained, which are 209.98 Pa and 177.69 Pa^2, respectively. The coefficient of variation (*CV*) of the bounded random variable is the ratio of the standard deviation and expectation of the bounded random variable. Here, the coefficient of variation of E_1^R can be computed, which is 6.35%. The λ^R and $c_{i,k}(k = 0,1,...)$ related to other bounded random variables in this numerical example can be calculated through the similar computational process. The *CV* of other bounded random variables are almost the same as that of E_1^R because all of them are assumed to have the same probabilistic distribution and α_R.

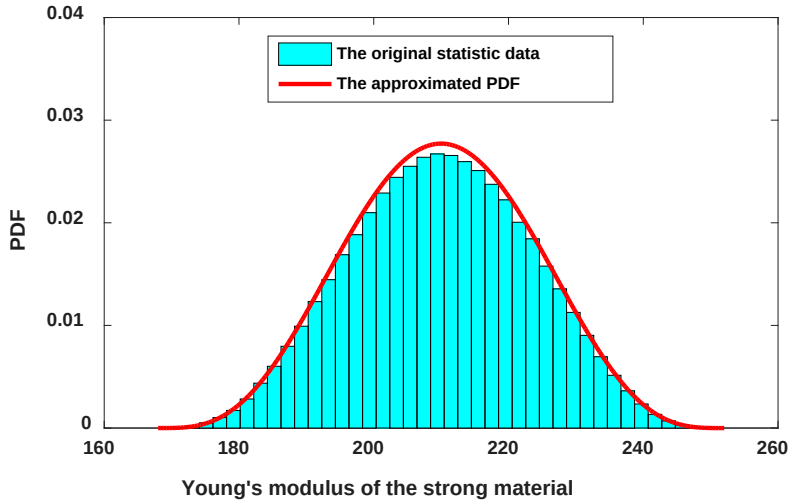

Fig. 3 The original statistic data and approximated PDF of the Young's modulus of strong material

The thickness of the periodical composite plate, the sound speed and density of the air are assumed to be independent interval variables owing to the limited probability distribution information. α_I denotes the uncertain level of these interval variables. The interval variables can be expressed as

$$\begin{aligned} t^I &= t\left[1-\alpha_I,\ 1+\alpha_I\right] \\ c^I &= c\left[1-\alpha_I,\ 1+\alpha_I\right] \\ \rho_f^I &= \rho_f\left[1-\alpha_I,\ 1+\alpha_I\right] \end{aligned} \tag{49}$$

In this paper, the results yielded by the integration of the MCM and scanning method are used as reference. The sampling number for interval variables and bounded random variables are 10^3 and 10^4, respectively. Therefore, the total sampling number is $10^3\times10^4=10^7$. All of the simulations are carried out by MATLAB R2017b on a 3.3GHz core(TM) i7-5820K.

The lower and upper bounds of the expectation and variance of the sound pressure amplitude along the central line are calculated by the HHSIPM and HGPEM when α_R=0.05 and α_I=0.1. The *CV* of E_1^R is computed, which is 1.63%. The considered frequencies are 100Hz and 150Hz. Theoretically, the efficiency of

HGPEM will decrease dramatically with the growth of the retained order of Gegenbauer polynomials. Reference [18] has established a retained order criterion for Gegenbauer polynomials expansion method. In this paper, with comprehensively considering the approximation accuracy and the computational cost, appropriate retained orders are chosen according to the retained order criterion. The retained orders of E_1, E_2, ρ_1, ρ_2, ρ_f^I t^I and c^I are [2, 2, 2, 2, 2, 3, 2]. Fig. 4 shows the results when the frequency is 100Hz. Fig. 5 shows the results when the frequency is 150Hz. The reference results are also plotted in Fig.4 and Fig. 5. The symbols “(L)” and “(U)” denote the lower and upper bound, respectively. It can be seen from Figs. 4 and 5 that the lower and upper bounds of the expectation and variance of the sound pressure amplitude along the central line calculated by both HGPEM and HHSIPM are close to the bounds of the reference results in two considered frequencies. This means that both HGPEM and HHSIPM can predict the periodical composite structural-acoustic system with multi-scale bounded hybrid uncertain parameters well when α_R is small. Nevertheless, by contrast, the bounds calculated by HGPEM match the reference results better than HHSIPM.

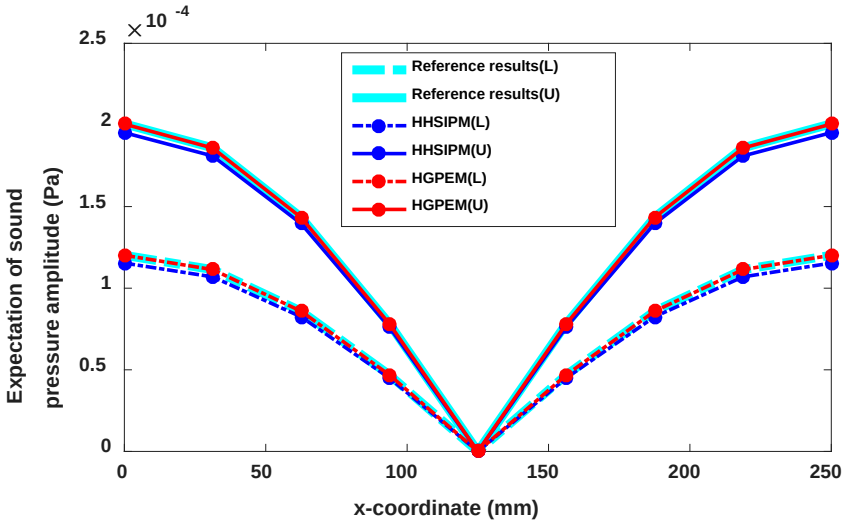

(a)

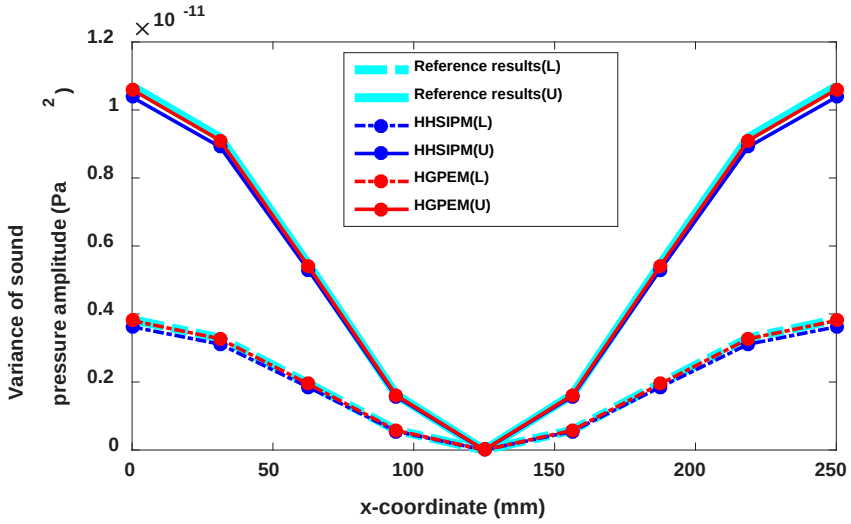

(b)

Fig. 4. The lower and upper bounds of the expectation and variance of the sound pressure amplitude along the central line (f=100Hz, α_R=0.05, α_I=0.1): (a) expectation (b) variance.

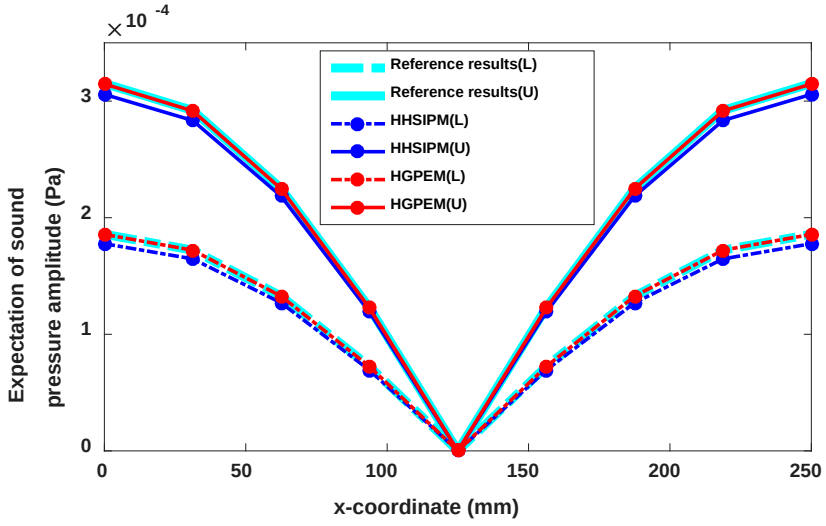

(a)

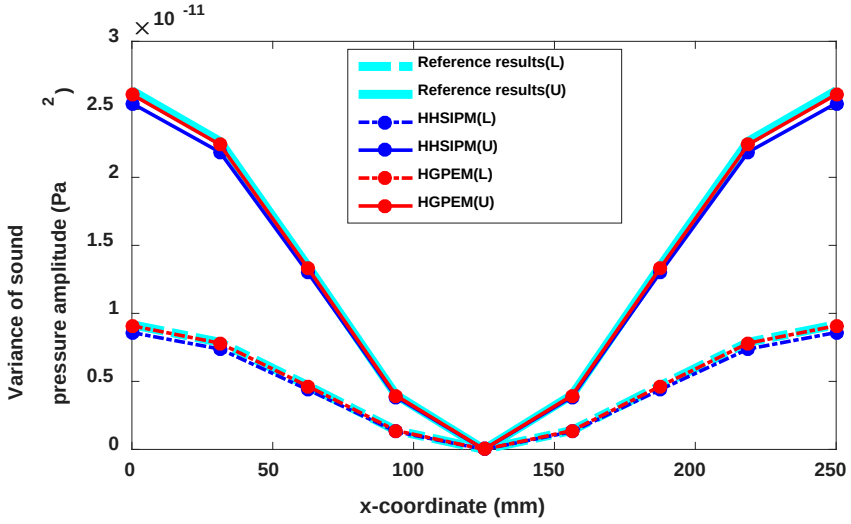

(b)

Fig. 5. The lower and upper bounds of the expectation and variance of the sound pressure amplitude along the central line (f=150Hz, α_R=0.05, α_I=0.1): (a) expectation (b) variance.

To investigate the accuracy of the HHSIPM and HGPEM for predicting the periodical composite structural-acoustic problem in more detail, the relative errors of the lower and upper bounds of the expectation and variance of the sound pressure amplitude along the central line are calculated and shown in Table 1 and Table 2 when f=100Hz. The symbol ‘‘RE’’ represents the relative errors. From Tables 1 and 2, we can see that the relative errors of HGPEM are much smaller than that of HHSIPM in terms of the lower and upper bounds of the expectation and variance. This indicates that the HGPEM has a better performance for predicting the periodical composite structural-acoustic problem with multi-scale bounded hybrid uncertainties compared with HHSIPM. The relative errors of HGPEM result from abandoning the higher order terms of Gegenbauer polynomials and the weighted least squares method. As for HHSIPM, the resource of relative errors is from neglecting the higher order terms of Taylor series and Neumann series. It can be concluded that the relative error of the Gegenbauer polynomials approximation is smaller than that of the first-order Taylor

expansion approximation with respect to same uncertain levels of bounded hybrid uncertain parameters. Besides, we can find that the relative errors of the bounds of variances are larger than that of the bounds of expectations. The reason of this phenomenon can be explained by the error propagation rule and the relationship between the expectation and variance.

Table 1 The lower and upper bounds of expectation of sound pressure amplitude along the central line (f=100Hz, α_R=0.05, α_I=0.1).

x-coordinate (mm)	Bounds	Reference results (Pa)	HGPEM (Pa)	RE	HHSIPM (Pa)	RE
0	LB	1.20E-04	1.20E-04	0.01%	1.15E-04	3.99%
	UB	2.01E-04	2.01E-04	0.07%	1.95E-04	2.69%
31.25	LB	1.11E-04	1.11E-04	0.01%	1.07E-04	3.98%
	UB	1.86E-04	1.86E-04	0.06%	1.81E-04	2.69%
62.5	LB	8.59E-05	8.59E-05	0.01%	8.25E-05	3.98%
	UB	1.43E-04	1.43E-04	0.06%	1.40E-04	2.69%
93.75	LB	4.68E-05	4.68E-05	0.01%	4.50E-05	3.98%
	UB	7.82E-05	7.82E-05	0.06%	7.61E-05	2.69%
156.25	LB	4.68E-05	4.68E-05	0.01%	4.50E-05	3.98%
	UB	7.82E-05	7.82E-05	0.06%	7.61E-05	2.69%
187.5	LB	8.59E-05	8.59E-05	0.01%	8.25E-05	3.98%
	UB	1.43E-04	1.43E-04	0.06%	1.40E-04	2.69%
218.75	LB	1.11E-04	1.11E-04	0.01%	1.07E-04	3.98%
	UB	1.86E-04	1.86E-04	0.06%	1.81E-04	2.69%
250	LB	1.20E-04	1.20E-04	0.01%	1.15E-04	3.99%
	UB	2.01E-04	2.01E-04	0.07%	1.95E-04	2.69%

Table 2 The lower and upper bounds of variance of sound pressure amplitude along the central line (f=100Hz, α_R=0.05, α_I=0.1).

x-coordinate (mm)	Bounds	Reference results (Pa^2)	HGPEM (Pa^2)	RE	HHSIPM (Pa^2)	RE
0	LB	3.84E-12	3.81E-12	0.76%	3.62E-12	5.54%
	UB	1.07E-11	1.06E-11	0.91%	1.04E-11	2.97%
31.25	LB	3.29E-12	3.27E-12	0.76%	3.11E-12	5.54%
	UB	9.10E-12	9.10E-12	0.91%	8.91E-12	2.97%
62.5	LB	1.96E-12	1.94E-12	0.76%	1.85E-12	5.54%
	UB	5.46E-12	5.41E-12	0.91%	5.30E-12	2.97%
93.75	LB	5.83E-13	5.78E-13	0.76%	5.50E-13	5.53%
	UB	1.61E-12	1.61E-12	0.91%	1.58E-12	2.97%
156.25	LB	5.83E-13	5.78E-13	0.76%	5.50E-13	5.53%
	UB	1.61E-12	1.61E-12	0.91%	1.58E-12	2.97%
187.5	LB	1.96E-12	1.94E-12	0.76%	1.85E-12	5.54%
	UB	5.46E-12	5.41E-12	0.91%	5.30E-12	2.97%

218.75	LB	3.29E-12	3.27E-12	0.76%	3.11E-12	5.54%
	UB	9.10E-12	9.10E-12	0.91%	8.91E-12	2.97%
250	LB	3.84E-12	3.81E-12	0.76%	3.62E-12	5.54%
	UB	1.07E-11	1.06E-11	0.91%	1.04E-11	2.97%

To investigate the effects of α_R on the accuracy of the HHSIPM and HGPEM, four α_R are considered, which are 0.1, 0.15, 0.2 and 0.3, respectively. The corresponding CV of E_1^R are calculated, that are 3.16%, 4.75%, 6.34% and 9.55%, respectively. The considered frequency is 100Hz. α_I is set as 0.1. The expectation of the sound pressure amplitude is independent of α_R according to the Eqs. (42) and (43). Therefore, the bounds of the expectation of the sound pressure amplitude in the cases with four different α_R are identical to the results as shown in Fig. 4(a). The lower and upper bounds of the variance of sound response amplitude along the central line obtained by the HHSIPM, HGPEM and the integration of the MCM and scanning method are shown in Fig. 6. It can be seen from Fig. 6 that the lower and upper bounds of variance of the sound pressure amplitude along the central line calculated by HGPEM match the reference results perfectly until α_R exceeds 0.2, whereas the lower and upper bounds calculated by HHSIPM are unacceptable from the beginning.

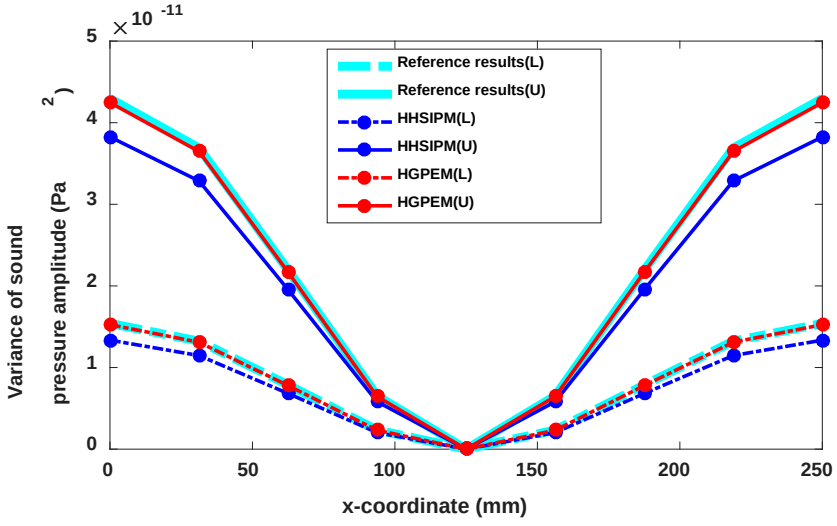

(a)

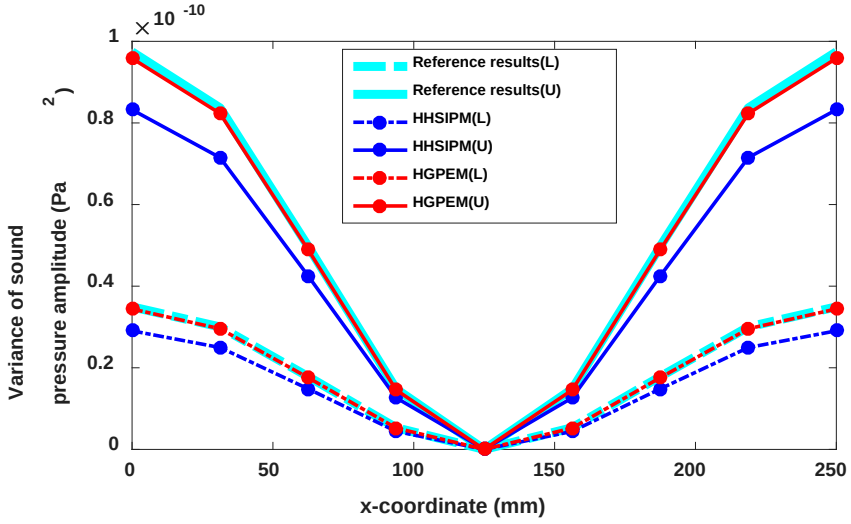

(b)

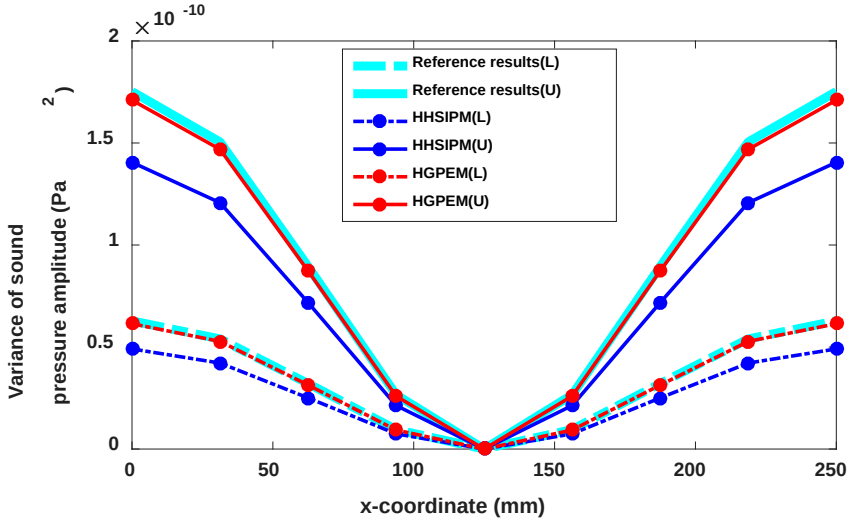

(c)

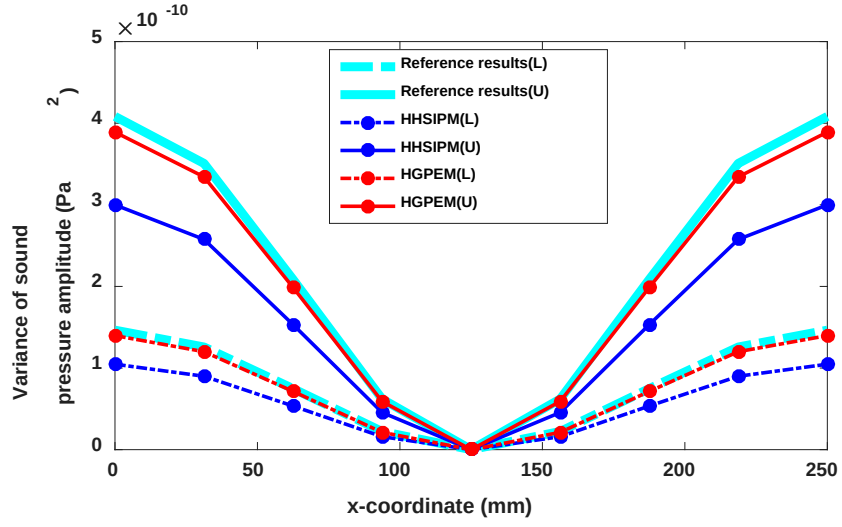

(d)

Fig. 6 The lower and upper bounds of the variance of sound pressure amplitude along the central line (f=100Hz, α_I=0.1): (a) α_R=0.1 (b) α_R =0.15 (c) α_R =0.2 (d) α_R =0.3.

The relative errors of the lower and upper bounds of variance of the sound pressure amplitude along the central line calculated by the HHSIPM and HGPEM are listed in Tables 3-6. It can be seen obviously from Tables 3-6 that the HGPEM can achieve a better accuracy than HHSIPM. For HGPEM, the relative errors of the obtained bounds of variance maintain at a very small value at four different considered α_R. However, the relative errors of bounds of variance calculated by the HHSIPM are tremendously large when α_R exceeds 0.1, which means that the results obtained by the HHSIPM are unreliable. This indicates that the presented HGPEM has a very good accuracy even if the α_R or *CV* is relatively large, while the accuracy of HHSIPM is acceptable only when the α_R or *CV* is very small. Overall speaking, the accuracies of both HHSIPM and HGPEM are affected by the α_R. The accuracy trend of these two methods is downwards with the α_R increasing. Compared with HGPEM, the HHSIPM is more vulnerable to the increase of α_R. Therefore, the HGPEM is verified to be a more reliable approach for the prediction of periodical composite structural-acoustic system with multi-scale bounded hybrid uncertain parameters.

Table 3 The lower and upper bounds of variance of sound pressure amplitude along the central line (f=100Hz, α_R=0.1, α_I=0.1).

x-coordinate (mm)	Bounds	Reference results (Pa^2)	HGPEM (Pa^2)	RE	HHSIPM (Pa^2)	RE
0	LB	1.54E-11	1.52E-11	1.00%	1.34E-11	13.30%
	UB	4.30E-11	4.25E-11	1.15%	3.83E-11	10.95%
31.25	LB	1.32E-11	1.31E-11	1.00%	1.15E-11	13.30%
	UB	3.65E-11	3.65E-11	1.15%	3.29E-11	10.94%
62.5	LB	7.87E-12	7.79E-12	1.00%	6.82E-12	13.30%
	UB	2.19E-11	2.17E-11	1.15%	1.95E-11	10.94%
93.75	LB	2.34E-12	2.32E-12	1.00%	2.03E-12	13.30%
	UB	6.45E-12	6.45E-12	1.15%	5.81E-12	10.94%
156.25	LB	2.34E-12	2.32E-12	1.00%	2.03E-12	13.30%
	UB	6.45E-12	6.45E-12	1.15%	5.81E-12	10.94%
187.5	LB	7.87E-12	7.79E-12	1.00%	6.82E-12	13.30%
	UB	2.19E-11	2.17E-11	1.15%	1.95E-11	10.94%

218.75	LB	1.32E-11	1.31E-11	1.00%	1.15E-11	13.30%
	UB	3.65E-11	3.65E-11	1.15%	3.29E-11	10.94%
250	LB	1.54E-11	1.52E-11	1.00%	1.34E-11	13.30%
	UB	4.30E-11	4.25E-11	1.15%	3.83E-11	10.95%

Table 4 The lower and upper bounds of variance of sound pressure amplitude along the central line (f=100Hz, α_R=0.15, α_I=0.1).

x-coordinate (mm)	Bounds	Reference results (Pa^2)	HGPEM (Pa^2)	RE	HHSIPM (Pa^2)	RE
0	LB	3.49E-11	3.44E-11	1.50%	2.91E-11	16.82%
	UB	9.74E-11	9.58E-11	1.65%	8.32E-11	14.56%
31.25	LB	3.00E-11	2.96E-11	1.50%	2.50E-11	16.82%
	UB	8.23E-11	8.23E-11	1.65%	7.15E-11	14.56%
62.5	LB	1.78E-11	1.76E-11	1.50%	1.48E-11	16.82%
	UB	4.98E-11	4.89E-11	1.65%	4.25E-11	14.56%
93.75	LB	5.31E-12	5.23E-12	1.50%	4.41E-12	16.82%
	UB	1.45E-11	1.45E-11	1.65%	1.26E-11	14.56%
156.25	LB	5.31E-12	5.23E-12	1.50%	4.41E-12	16.82%
	UB	1.45E-11	1.45E-11	1.65%	1.26E-11	14.56%
187.5	LB	1.78E-11	1.76E-11	1.50%	1.48E-11	16.82%
	UB	4.98E-11	4.89E-11	1.65%	4.25E-11	14.56%
218.75	LB	3.00E-11	2.96E-11	1.50%	2.50E-11	16.82%
	UB	8.23E-11	8.23E-11	1.65%	7.15E-11	14.56%
250	LB	3.49E-11	3.44E-11	1.50%	2.91E-11	16.82%
	UB	9.74E-11	9.58E-11	1.65%	8.32E-11	14.56%

Table 5 The lower and upper bounds of variance of sound pressure amplitude along the central line (f=100Hz, α_R=0.2, α_I=0.1).

x-coordinate (mm)	Bounds	Reference results (Pa^2)	HGPEM (Pa^2)	RE	HHSIPM (Pa^2)	RE
0	LB	6.28E-11	6.14E-11	2.25%	4.91E-11	21.91%
	UB	1.75E-10	1.71E-10	2.40%	1.41E-10	19.79%
31.25	LB	5.40E-11	5.27E-11	2.25%	4.21E-11	21.91%
	UB	1.47E-10	1.47E-10	2.40%	1.21E-10	19.79%
62.5	LB	3.21E-11	3.14E-11	2.25%	2.51E-11	21.91%
	UB	8.95E-11	8.73E-11	2.40%	7.18E-11	19.78%
93.75	LB	9.54E-12	9.33E-12	2.25%	7.45E-12	21.90%
	UB	2.60E-11	2.60E-11	2.40%	2.13E-11	19.78%
156.25	LB	9.54E-12	9.33E-12	2.25%	7.45E-12	21.90%
	UB	2.60E-11	2.60E-11	2.40%	2.13E-11	19.78%
187.5	LB	3.21E-11	3.14E-11	2.25%	2.51E-11	21.91%
	UB	8.95E-11	8.73E-11	2.40%	7.18E-11	19.78%
218.75	LB	5.40E-11	5.27E-11	2.25%	4.21E-11	21.91%
	UB	1.47E-10	1.47E-10	2.40%	1.21E-10	19.79%
250	LB	6.28E-11	6.14E-11	2.25%	4.91E-11	21.91%
	UB	1.75E-10	1.71E-10	2.40%	1.41E-10	19.79%

Table 6 The lower and upper bounds of variance of sound pressure amplitude along the central line

(f=100Hz, α_R=0.3, α_I=0.1).

x-coordinate (mm)	Bounds	Reference results (Pa^2)	HGPEM (Pa^2)	RE	HHSIPM (Pa^2)	RE
0	LB	1.46E-10	1.40E-10	4.56%	1.05E-10	28.49%
	UB	4.08E-10	3.89E-10	4.71%	3.00E-10	26.54%
31.25	LB	1.26E-10	1.20E-10	4.56%	8.99E-11	28.49%
	UB	3.34E-10	3.34E-10	4.71%	2.58E-10	26.54%
62.5	LB	7.48E-11	7.14E-11	4.56%	5.35E-11	28.49%
	UB	2.09E-10	1.99E-10	4.71%	1.53E-10	26.54%
93.75	LB	2.22E-11	2.12E-11	4.56%	1.59E-11	28.48%
	UB	5.91E-11	5.91E-11	4.71%	4.55E-11	26.54%
156.25	LB	2.22E-11	2.12E-11	4.56%	1.59E-11	28.48%
	UB	5.91E-11	5.91E-11	4.71%	4.55E-11	26.54%
187.5	LB	7.48E-11	7.14E-11	4.56%	5.35E-11	28.49%
	UB	2.09E-10	1.99E-10	4.71%	1.53E-10	26.54%
218.75	LB	1.26E-10	1.20E-10	4.56%	8.99E-11	28.49%
	UB	3.34E-10	3.34E-10	4.71%	2.58E-10	26.54%
250	LB	1.46E-10	1.40E-10	4.56%	1.05E-10	28.49%
	UB	4.08E-10	3.89E-10	4.71%	3.00E-10	26.54%

The effects of α_I on the accuracy of the HHSIPM and the HGPEM are also investigated. The considered frequency is 100Hz. Fig. 7 depicts lower and upper bounds of expectation and variance of the sound response amplitude along the central line calculated by the HHSIPM, HGPEM and the integration of the MCM and scanning method when α_R=0.05 and α_I=0.2. The effects of α_I on the accuracy of HHSIPM and HGPEM in terms of variance can be found by comparing Figs. 4(b) and 7(b). It is obvious that the bounds of variance calculated by HGPEM still have a good agreement with the reference results when α_I increases to 0.2. However, the bounds calculated by the HHSIPM have a large deviation with the reference results when α_I increases to 0.2. As for expectation, through comparing Figs. 4(a) and 7(a) it can be found that the results of the expectation obtained by HGPEM still have a good accuracy at large uncertain level of the interval variables, while the accuracy of the results for expectation calculated by HHSIPM is not satisfactory.

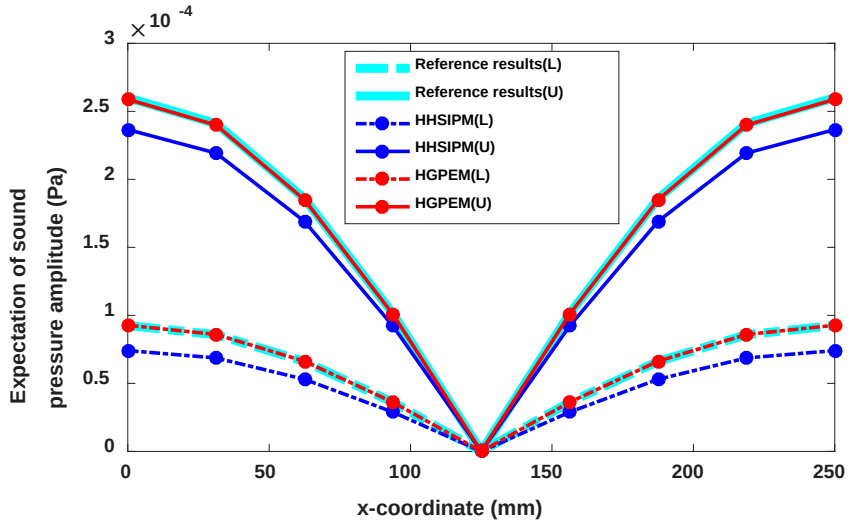

(a)

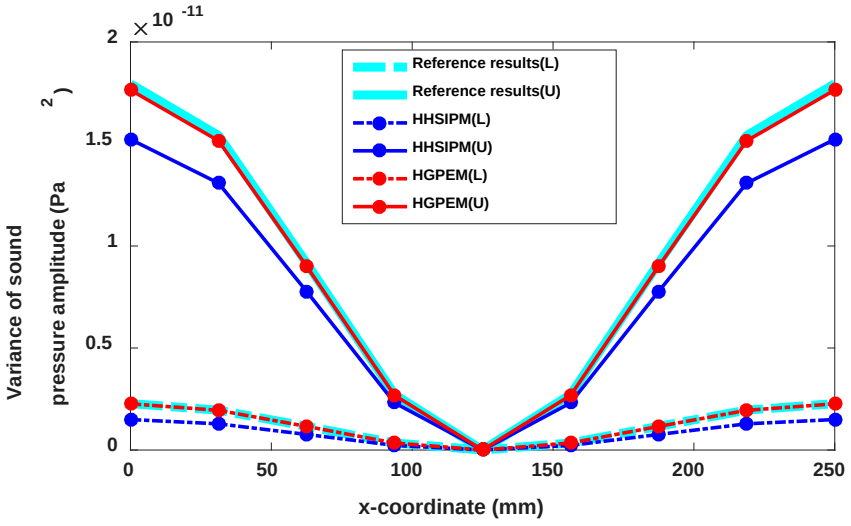

(b)

Fig. 7 The lower and upper bounds of the expectation and variance of sound pressure amplitude along the central line (f=100Hz, α_R=0.05, α_I=0.2): (a) expectation (b) variance

Fig. 8 plots the lower and upper bounds of the expectation and variance of the sound pressure amplitude at the point A calculated by HHSIPM, HGPEM and the integration of the MCM and scanning method within an interval frequency ranging from 50 Hz to 300 Hz when α_R=0.2 and α_I=0.2. It can be seen from Fig. 8 that the bounds calculated by HGPEM match the reference results perfectly within the interval frequency, whereas the bounds calculated by HHSIPM have larger disagreement with the reference results. Therefore, the effectiveness of HGPEM is further verified when

it is used to conduct the hybrid interval and random analysis for periodical composite structural-acoustic system with multi-scale bounded hybrid uncertain parameters.

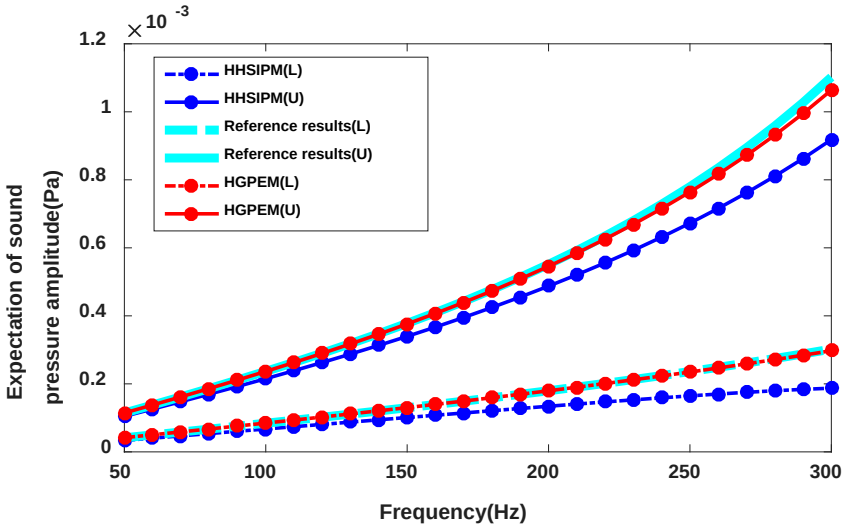

(a)

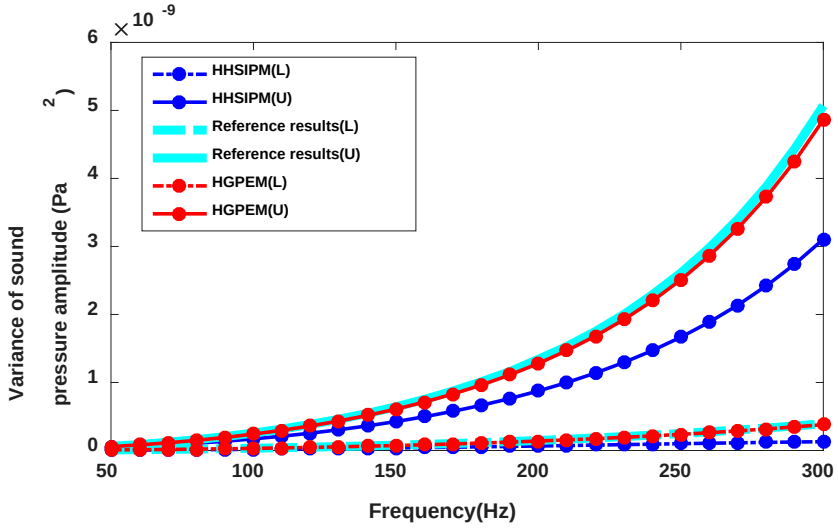

(b)

Fig. 8 The lower and upper bounds of the expectation and variance of sound pressure amplitude at point A (50-300 Hz): (a) expectation (b) variance.

Table 7 lists the execution time of the integration of the MCM and scanning method, HHSIPM and HGPEM, respectively. It can be obviously found that the time execution time of HGPEM is much less than that of the integration of the MCM and scanning method and a bit longer than that of HHSIPM. Actually, when the input uncertain level increasing, more execution time is needed for predicting periodical

composite structural-acoustic system with multi-scale bounded hybrid uncertain parameters through HGPEM. The reason of this is that higher retained order of HGPEM is needed for reducing the relative error of predicting periodical composite structural-acoustic system with multi-scale larger uncertain level. Nevertheless, compared to the integration of the MCM and scanning method, the execution time of the HGPEM is significantly lower. Furthermore, the HGPEM is more reliable and has a better accuracy than the HHSIPM though the execution time of HHSIPM is the least.

Table 7 The execution time of the integration of the MCM and scanning method, HHSIP and HGPEM.

Methods	Reference approach	HHSIPM	HGPEM
Time(s)	17280	54.3	365.4

6.2. An automobile passenger compartment

An automobile passenger compartment with a flexible roof panel is shown in Fig. 9. The flexible thin roof constructed of periodic uniform unidirectional fiber reinforced composites is excited by a harmonic point force F=1 N at its middle point. The roof panel's thickness is 1 mm. All edges of the plate are fixed. The density and the sound speed of the air are 1.21 kg/m^3 and 340.5 m/s. Node A is located near the left ear of the driver to observe the sound pressure amplitude in the acoustic domain. The RVE is composed of two prescribed materials, which are the same as those in first numerical example. The Young's modulus and the mass density of the two prescribed

materials are defined to be independent bounded random variables. The Young's modulus and the mass density of the strong material are assumed to be $E_1^R=E_1[1-\alpha_R, 1+\alpha_R]$ and $\rho_1^R=\rho_1[1-\alpha_R, 1+\alpha_R]$, respectively. The Young's modulus and mass density of the soft material are $E_2^R=E_2[1-\alpha_R, 1+\alpha_R]$ and $\rho_2^R=\rho_2[1-\alpha_R, 1+\alpha_R]$, respectively. All of the bounded random variables in this numerical example follow the same probabilistic distribution as those in first numerical example. The thickness of the flexible roof, the sound speed and density of the air are defined to be independent interval variables, that are $t^I=1[1-\alpha_I, 1+\alpha_I]$ mm, $c^I=340.5[1-\alpha_I, 1+\alpha_I]$ m/s and $\rho_f^I=1.21[1-\alpha_I, 1+\alpha_I]$ kg/m^3, respectively. The HHSIPM, HGPEM and the integration of the MCM and scanning method are used to calculate the upper and lower bounds of the expectation and variance of the sound response amplitude at node A. The retained orders of Gegenbauer polynomials related to bounded hybrid uncertain parameters are the same as those in the first numerical example. All of these simulations are carried out by MATLAB R2017b on a 3.3GHz core(TM) i7-5820K. The sampling number for interval variables and bounded random variables is the same as that of the first numerical example.

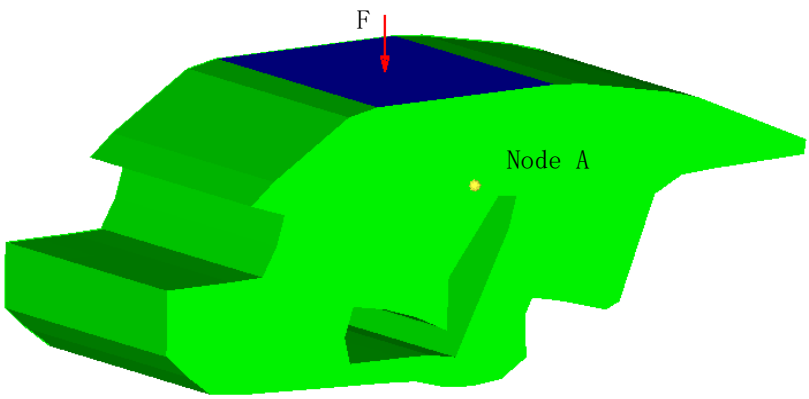

Fig. 9 An automobile passenger compartment

The lower and upper bounds of the expectation and variance of sound pressure amplitude at node A calculated by the HHSIPM, HGPEM and the integration of the MCM and scanning method in the frequency band 50–300 Hz are plotted in Fig. 10 when α_R=0.225 and α_I=0.2. Here, the coefficient of variation of E_1^R is computed, which is 7.53%. It can be seen from Fig. 10 that the bounds of the expectation and variance obtained by HGPEM match the reference results well within the interval frequency. However, the bounds of the expectation and variance computed by HHSIPM deviate from the reference results obviously in the frequency band. The relative errors of the lower and upper bounds of expectation and variance of the sound pressure amplitude at node A calculated by the HHSIPM and HGPEM are listed in Tables 8 and 9. From Tables 8 and 9, we can see that the relative errors of HHSIPM are a little bigger than that of HGPEM in terms of the lower and upper bounds of the expectation. However, the relative errors of variance calculated by HHSIPM is absolutely unacceptable, while the relative errors calculated by HGPEM maintain at a reasonable level. This further indicates that the HGPEM has a better performance for predicting the periodical composite structural-acoustic problem with multi-scale bounded hybrid uncertainties compared with HHSIPM. Therefore, the presented HGPEM can achieve high accuracy for the hybrid interval and random analysis of periodical composite structural-acoustic system with multi-scale bounded hybrid uncertain parameters in practical engineering problems.

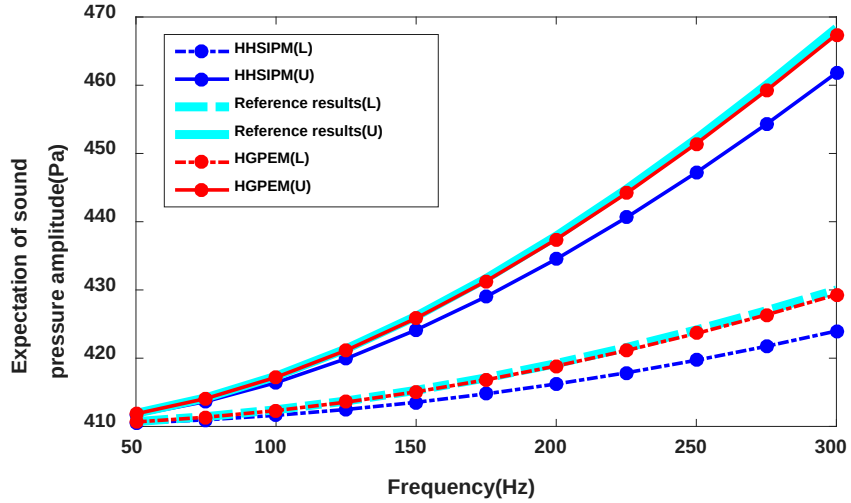

(a)

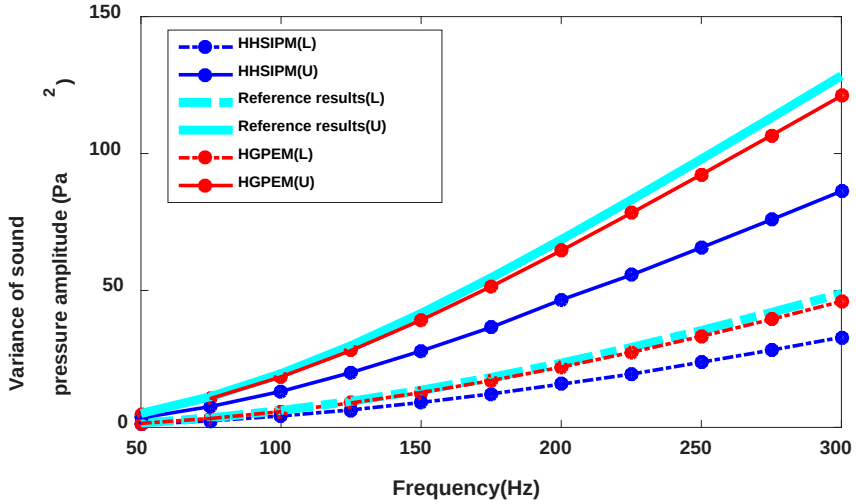

(b)

Fig. 10 The lower and upper bounds of the expectation and variance of sound pressure amplitude at node A in the passenger compartment (50-300 Hz): (a) expectation (b) variance.

Table 8 The lower and upper bounds of the expectation of sound pressure amplitude at node A in the passenger compartment (50-300 Hz).

Frequency (Hz)	Bounds	Reference results (Pa)	HGPEM (Pa)	RE	HHSIPM (Pa)	RE
50	LB	410.64	410.62	0.00%	410.49	0.04%
	UB	411.83	411.82	0.00%	411.66	0.04%
75	LB	411.31	411.28	0.01%	410.96	0.08%
	UB	414.07	414.05	0.00%	413.65	0.10%
100	LB	412.26	412.20	0.01%	411.63	0.15%
	UB	417.16	417.14	0.01%	416.42	0.18%
125	LB	413.46	413.38	0.02%	412.48	0.24%
	UB	421.07	421.04	0.01%	419.92	0.27%
150	LB	414.93	414.81	0.03%	413.53	0.34%
	UB	425.76	425.71	0.01%	424.14	0.38%
175	LB	416.65	416.49	0.04%	414.78	0.45%
	UB	431.17	431.10	0.02%	429.02	0.50%

200	LB	418.62	418.41	0.05%	416.22	0.57%
	UB	437.25	437.16	0.02%	434.52	0.62%
225	LB	420.83	420.57	0.06%	417.86	0.71%
	UB	443.94	443.82	0.03%	440.60	0.75%
250	LB	423.27	422.96	0.07%	419.70	0.84%
	UB	451.18	451.04	0.03%	447.21	0.88%
275	LB	425.94	425.58	0.08%	421.74	0.99%
	UB	458.91	458.73	0.04%	454.29	1.01%
300	LB	428.83	428.41	0.10%	423.98	1.13%
	UB	467.06	466.85	0.05%	461.80	1.13%

Table 9 The lower and upper bounds of the variance of sound pressure amplitude at node A in the passenger compartment (50-300 Hz)

Frequency (Hz)	Bounds	Reference results (Pa^2)	HGPEM (Pa^2)	RE	HHSIPM (Pa^2)	RE
50	LB	1.56	1.44	7.61%	1.12	28.39%
	UB	5.14	4.77	7.27%	3.47	32.59%
75	LB	3.48	3.21	7.79%	2.40	31.19%
	UB	11.40	10.57	7.32%	7.65	32.87%
100	LB	6.15	5.67	7.89%	4.17	32.17%
	UB	19.86	18.37	7.50%	13.14	33.81%
125	LB	9.53	8.77	7.97%	6.39	32.98%
	UB	30.24	27.95	7.56%	19.96	34.00%
150	LB	13.59	12.50	8.02%	9.10	33.04%
	UB	42.22	39.00	7.63%	27.80	34.14%
175	LB	18.29	16.76	8.36%	12.23	33.13%
	UB	55.47	51.15	7.79%	36.45	34.29%
200	LB	23.58	21.51	8.80%	15.75	33.20%
	UB	69.65	64.18	7.86%	45.71	34.38%
225	LB	29.42	26.79	8.92%	19.45	33.89%
	UB	84.47	77.77	7.94%	54.95	34.95%
250	LB	35.74	32.51	9.04%	23.61	33.95%
	UB	99.69	91.70	8.02%	64.73	35.07%
275	LB	42.49	38.51	9.36%	28.00	34.10%
	UB	115.15	105.81	8.11%	74.33	35.45%
300	LB	49.62	44.92	9.48%	32.63	34.25%
	UB	130.77	120.02	8.22%	84.01	35.75%

7. Conclusion

This paper presents two hybrid interval and random analysis methods for the prediction of periodical composite structural-acoustic systems with multi-scale uncertain-but-bounded parameters. The bounded hybrid uncertain model is employed to treat the multi-scale uncertain-but-bounded parameters involved in the periodical

composite structural-acoustic system, in which the interval variables and the bounded random variables exist simultaneously. In the periodical composite structural-acoustic system, the equivalent macro constitutive matrix and average mass density of the microstructure are calculated through the homogenization method. Based on the HFEM and conventional first-order Taylor series expansion, the HHSIPM is developed for the analysis of periodical composite structural-acoustic system with multi-scale bounded hybrid uncertain parameters. By incorporating the Gegenbauer polynomial approximation theory into the HFEM, the HGPEM is also proposed to calculate the bounds of expectation and variance of the sound pressure response. Numerical results for a hexahedral box and an automobile passenger compartment indicate that the proposed HGPEM has a better accuracy compared with HHSIPM in predicting the periodical composite structural-acoustic systems with multi-scale bounded hybrid uncertain parameters. Besides, the HGPEM can achieve a desirable accuracy even if the uncertain levels of the multi-scale bounded hybrid uncertain parameters are relatively large, whereas, the accuracy of the HHSIPM is acceptable only when the uncertain levels are very small. Therefore, the HGPEM is verified to be a more reliable and promising approach for the prediction of periodical composite structural-acoustic system with multi-scale bounded hybrid uncertain parameters.

Acknowledgments

The paper is supported by the Key Project of Science and Technology of Changsha (Grant No. KQ1703028) and the Fundamental Research Funds for the Central Universities (531107051148). The author would also like to thank reviewers for their

valuable suggestions.

References

[1] Hashin Z, Rosen BW. The elastic moduli of fiber-reinforced materials. Journal of applied mechanics-transactions of the ASME 21 (1964) 223-232.

[2] Tanaka S, Ichikawa M, Akita S. A probabilistic investigation of fatigue life and cumulative cycle ratio. Engineering Fracture Mechanics 20 (1984) 501-513.

[3] Hollister SJ, Kikuchi N, A Comparison of Homogenization and Standard Mechanics Analyses for Periodic Porous Composites. Computational Mechanics, 10 (1992) 73–95.

[4] Hassani B, Hinton E, A Review of Homogenization and Topology Optimization I - Homogenization Theory for Media with Periodic Structure. Computer & Structures, 69 (1998) 707-717.

[5] Hassani B, Hinton E, A Review of Homogenization and Topology Optimization II - Analytical and Numerical Solution of Homogenization Equations. Computer & Structures, 69 (1998) 719-738.

[6] N. Chen, D. Yu, B. Xia, J. Liu, Z. Ma, Homogenization-based interval analysis for structural-acoustic problem involving periodical composites and multi-scale uncertain-but-bounded parameters. Journal of the Acoustical Society of America 141 (4) (2017) 2768.

[7] M.P. Bendsøe, O. Sigmund, Topology Optimization: Theory, Methods, and

Applications. Springer, 2003.

[8] L.Wang, X. Wang, Y. Li, G. Lin, Z. Qiu, Structural time - dependent reliability assessment of the vibration active control system with unknown-but-bounded uncertainties. Structural Control & Health Monitoring 24 (10) (2017) e1965.

[9] L.Wang, C. Xiong, X. Wang, Y. Li, M. Xu, Hybrid time-variant reliability estimation for active control structures under aleatory and epistemic uncertainties. Journal of Sound & Vibration 419 (2018) 469-492.

[10] L.Wang, X. Wang, Y. Yang, Y. Li, X. Chang, Active force control of structure-borne sound based on robust optimization subjected to an irregular cavity with uncertainties. Aerospace Science & Technology 73 (2018) 318-331.

[11] B. Xia, D. Yu, J. Liu, Interval and subinterval perturbation methods for a structural-acoustic system with interval parameters. Journal of Fluids and Structures 38 (2013) 146–163.

[12] B. Xia, D. Yu, J, Liu, Hybrid uncertain analysis for structural–acoustic problem with random and interval parameters. Journal of Sound and Vibration 332 (2013) 2701–2720.

[13] B. Xia, D. Yu, An interval random perturbation method for structural-acoustic system with hybrid uncertain parameters. International Journal for Numerical Methods in Engineering 97 (3) (2014) 181-206.

[14] M. Xu, Z. Qiu, X. Wang, Uncertainty propagation in SEA for structural–acoustic coupled systems with non-deterministic parameters. Journal of Sound and Vibration. 333 (17) (2014) 3949-3965.

[15] H. Yin, D. Yu, L. Hui, S. Yin, B. Xia, Hybrid finite element/statistical energy method for mid-frequency analysis of structure−acoustic systems with interval parameters. Journal of Sound and Vibration 353 (2015) 181-204.

[16] B. Xia, S. Yin, D. Yu, A new random interval method for response analysis of structural–acoustic system with interval random variables. Applied Acoustics 99 (2015) 31-42.

[17] N. Chen, D. Yu, B. Xia, M. Beer, Uncertainty analysis of a structural–acoustic problem using imprecise probabilities based on p-box representations. Mechanical Systems and Signal Processing 80 (2016) 45-57.

[18] S. Yin, D. Yu, H. Yin, B. Xia, Interval and random analysis for structure–acoustic systems with large uncertain-but-bounded parameters. Computer Methods in Applied Mechanics and Engineering 305 (2016) 910-935.

[19] M. Xu, J. Du, C. Wang, Y. Li, Hybrid uncertainty propagation in structural-acoustic systems based on the polynomial chaos expansion and dimension-wise analysis. Computer Methods in Applied Mechanics & Engineering 320 (2017) 198-217.

[20] J.E. Hurtado, A.H. Barbat, Monte carlo techniques in computational stochastic mechanics. Archives of Computational Methods in Engineering 5 (1) (1998) 3.

[21] P.D. Spanos, A. Kontsos, A multiscale Monte Carlo finite element method for determining mechanical properties of polymer nanocomposites. Probabilistic Engineering Mechanics 23(4) (2008) 456–470.

[22] B. Rong, X. Rui, L. Tao, Perturbation finite element transfer matrix method for random eigenvalue problems of uncertain structures. Journal of applied mechanics-transactions of the ASME 79 (2) (2012) 1005.

[23] O. Cavdar, A. Bayraktar, A. Cavdar, S. Adanur, Perturbation based Stochastic finite element analysis of the structural systems with composite sections under earthquake forces. Steel and Composite Structures 8 (2) (2008) 129–144.

[24] M. Kaminski, A generalized stochastic perturbation technique for plasticity problems, Computational Mechanics 45 (4) (2010) 349–361.

[25] B. Lazarov, M. Schevenels, O. Sigmund, Topology optimization with geometric uncertainties by perturbation techniques. International Journal for Numerical Methods in Engineering 90 (11) (2012) 1321–1336.

[26] R.G. Ghanem, P.D. Spanos, Stochastic Finite Elements. Springer-Verlag (1991) 224.

[27] N. Wiener, The homogeneous chaos, American Journal of Mathematics 60 (4) (1938) 897-936.

[28] A. Nouy, Recent developments in spectral stochastic methods for the numerical solution of stochastic partial differential equations. Archives of Computational Methods in Engineering 16 (2009) 251–285.

[29] M.D. Shields, G. Deodatis, A simple and efficient methodology to approximate a general non-Gaussian stationary stochastic vector process by a translation process with applications in wind velocity simulation. Probabilistic Engineering Mechanics

31 (2013) 19–29.

[30] G. Stefanou, The stochastic finite element method: past, present and future. Computer Methods in Applied Mechanics and Engineering 198 (9–12) (2009) 1031–1051.

[31] W. Gao, Stochastically optimal active control of a smart truss structure under stationary random excitation. Journal of Sound and Vibration 290 (3) (2006) 1256–1268.

[32] D. Moens, D. Vandepitte, A survey of non-probabilistic uncertainty treatment in finite element analysis. Computer Methods in Applied Mechanics & Engineering 194 (2005) 1527–1555.

[33] Z.P. Qiu, S.H. Chen, I. Elishakoff, Bounds of eigenvalues for structures with an interval description of uncertain-but-non-random parameters, Chaos Solitons & Fractals 7 (3) (1996) 425–434.

[34] J. Wu, Y. Zhang, L. Chen, Z. Luo, A Chebyshev interval method for nonlinear dynamic systems under uncertainty. Applied Mathematical Modelling 37 (6) (2013) 4578–4591.

[35] I. Elishakoff, P. Colombi, Combination of probabilistic and convex models of uncertainty when scarce knowledge is present on acoustic excitation parameters. Computer Methods in Applied Mechanics & Engineering 104 (2) (1993) 187–209.

[36] J. Wang, Z.P. Qiu, The reliability analysis of probabilistic and interval hybrid structural system. Applied Mathematical Modelling 34 (11) (2010) 3648–3658.

[37] C. Jiang, W.X. Li, X. Han, L.X. Liu, P.H. Le, Structural reliability analysis based on random distributions with interval parameters. Computers & Structures 89 (2011) 2292–2302.

[38] G. Muscolino, A. Sofi, Response statistics of linear structures with uncertain-but-bounded parameters under Gaussian stochastic input. International Journal of Structural Stability & Dynamics 11 (2011) 775–804.

[39] N. Chen, D. Yu, B. Xia, Hybrid uncertain analysis for the prediction of exterior acoustic field with interval and random parameters. Computers & Structures 141 (2014) 9–18.

[40] W. Gao, D. Wu, C. Song, F. Tin-Loi, X. Li, Hybrid probabilistic interval analysis of bar structures with uncertainty using a mixed perturbation Monte-Carlo method. Finite Elements in Analysis & Design 47 (2011) 643–652.

[41] J. Wu, Z. Luo, N. Zhang, Y. Zhang, A new uncertain analysis method and its application in vehicle dynamics. Mechanical Systems and Signal Processing 50 (2015) 659–675.

[42] S. Yin, D. Yu, H. Yin, B. Xia, A unified method for the response analysis of interval/random variable models of acoustic fields with uncertain- but- bounded parameters. International Journal for Numerical Methods in Engineering 111 (2017).

[43] M.P. Bendsoe, N. Kikuchi, Generating optimal topologies in structural design using a homogenization method, Computer Methods in Applied Mechanics and

Engineering 71 (2) (1988) 197-224.

[44] N. Chen, D. Yu, B. Xia, Hybrid uncertain analysis for the prediction of exterior acoustic field with interval and random parameters. Computers & Structures 141 (2014) 9-18.

[45] S. Adhikari, A reduced spectral function approach for the stochastic finite element analysis. Computer Methods in Applied Mechanics & Engineering 200 (21–22) (2011) 1804-1821.

[46] C.L. Wu, X.P. Ma, T. Fang, A complementary note on gegenbauer polynomial approximation for random response problem of stochastic structure. Probabilistic Engineering Mechanics 21 (4) (2006) 410-419.

[47] G. Szego, Orthogonal Polynomials. American Mathematical Society (1938).

[48] J. Liu, X. Sun, X. Han, C. Jiang, D. Yu, Dynamic load identification for stochastic structures based on Gegenbauer polynomial approximation and regularization method, Mechanical Systems and Signal Processing (2015) 35–54.